

An Inositolphosphorylceramide Synthase Is Involved in Regulation of Plant Programmed Cell Death Associated with Defense in *Arabidopsis*

Wenming Wang,^{a,1} Xiaohua Yang,^{a,1} Samantha Tangchaiburana,^a Roland Ndeh,^a Jonathan E. Markham,^b Yoseph Tsegaye,^c Teresa M. Dunn,^c Guo-Liang Wang,^d Maria Bellizzi,^d James F. Parsons,^e Danielle Morrissey,^f Janis E. Bravo,^f Daniel V. Lynch,^f and Shunyuan Xiao^{a,2}

^a Center for Biosystems Research, University of Maryland Biotechnology Institute, Rockville, Maryland 20850

^b Donald Danforth Plant Science Center, St. Louis, Missouri 63132

^c Department of Biochemistry and Molecular Biology, Uniformed Services University of the Health Sciences, Bethesda, Maryland 20814

^d Department of Plant Pathology, The Ohio State University, Columbus Ohio 43210

^e Center for Advanced Research in Biotechnology, University of Maryland Biotechnology Institute, Rockville, Maryland 20850

^f Department of Biology, Williams College, Williamstown, Massachusetts 01267

The *Arabidopsis thaliana* resistance gene *RPW8* triggers the hypersensitive response (HR) to restrict powdery mildew infection via the salicylic acid-dependent signaling pathway. To further understand how *RPW8* signaling is regulated, we have conducted a genetic screen to identify mutations enhancing *RPW8*-mediated HR-like cell death (designated *erh*). Here, we report the isolation and characterization of the *Arabidopsis erh1* mutant, in which the *At2g37940* locus is knocked out by a T-DNA insertion. Loss of function of *ERH1* results in salicylic acid accumulation, enhanced transcription of *RPW8* and *RPW8*-dependent spontaneous HR-like cell death in leaf tissues, and reduction in plant stature. Sequence analysis suggests that *ERH1* may encode the long-sought *Arabidopsis* functional homolog of yeast and protozoan inositolphosphorylceramide synthase (IPCS), which converts ceramide to inositolphosphorylceramide. Indeed, *ERH1* is able to rescue the yeast *aur1* mutant, which lacks the IPCS, and the *erh1* mutant plants display reduced (~53% of wild type) levels of leaf IPCS activity, indicating that *ERH1* encodes a plant IPCS. Consistent with its biochemical function, the *erh1* mutation causes ceramide accumulation in plants expressing *RPW8*. These data reinforce the concept that sphingolipid metabolism (specifically, ceramide accumulation) plays an important role in modulating plant programmed cell death associated with defense.

INTRODUCTION

Plants have evolved disease resistance (*R*) genes to protect themselves from the attack of various pathogens. Characterized plant *R* genes can be divided into several classes based on their predicted protein structures and functions. The majority of them encode proteins containing a nucleotide binding site and leucine-rich repeat motifs (NB-LRR). These *R* proteins can be further subdivided into two major subclasses: those having an N-terminal coiled-coil (CC) domain and those containing an N-terminal domain resembling the cytoplasmic signaling domain of the *Drosophila* Toll and human Interleukin-1 (TIR) transmembrane receptors (Dangl and Jones, 2001).

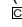
The *Arabidopsis thaliana* *R* gene *RPW8* mediates broad-spectrum resistance to powdery mildew (Xiao et al., 2001). The *RPW8* locus is not present in *Arabidopsis* accession Columbia (Col-0), but accession Ms-0 contains two homologous, functional *R* genes named *RPW8.1* and *RPW8.2* (Xiao et al., 2001). These two genes are hereafter referred to as *RPW8* unless otherwise indicated. *RPW8* is unique among the cloned *R* genes because the deduced *RPW8* proteins contain an N-terminal transmembrane domain and one to two CCs and show no significant homology to other proteins, thus belonging to a unique *R* protein category (Dangl and Jones, 2001; Xiao et al., 2001). *RPW8* confers broad-spectrum resistance to powdery mildew isolates from four *Golovinomyces* species that are capable of infecting hundreds of dicot plant species, including many economically important crops (Xiao et al., 2001). *RPW8*-mediated resistance is associated with typical plant defense responses similar to those regulated by classic *NB-LRR* genes, including rapid generation of H₂O₂ at the fungal penetration sites, induction of pathogenesis-related (*PR*) genes, and triggering of the hypersensitive response (HR), a form of programmed cell death (PCD) at the site of infection.

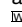
The HR is often, although not always, associated with defenses activated by various plant *R* genes against biotrophic and

¹ These authors contributed equally to this work.

² Address correspondence to xiao@umbi.umd.edu.

The author responsible for distribution of materials integral to the findings presented in this article in accordance with the policy described in the Instructions for Authors (www.plantcell.org) is: Shunyuan Xiao (xiao@umbi.umd.edu).

 Some figures in this article are displayed in color online but in black and white in the print edition.

 Online version contains Web-only data.

www.plantcell.org/cgi/doi/10.1105/tpc.108.060053

hemibiotrophic pathogens. HR-like cell death has been used as a phenotypic readout of defense activation in many genetic screens for identifying components that negatively regulate plant defense signaling (Lorrain et al., 2003). Many *Arabidopsis* mutants with spontaneous HR-like lesions and/or constitutive activation of defense marker genes have been isolated, and some of the responsible genes may indeed act as negative regulators in pathways leading to PCD activation and defense responses (Hammond-Kosack and Parker, 2003; Lorrain et al., 2003). Such studies have implicated many different cellular processes in the regulation of plant PCD pathway(s) that may be associated with plant defenses, including chlorophyll metabolism (Mach et al., 2001; Pruzinska et al., 2003), ion channeling (Clough et al., 2000; Balague et al., 2003; Jurkowski et al., 2004), protein phosphorylation/dephosphorylation (Frye et al., 2001; He et al., 2004), fatty acid homeostasis and modification (Kachroo et al., 2001, 2004), callose synthesis (Nishimura et al., 2003), superoxide production (Kliebenstein et al., 1999; Epple et al., 2003), lipid metabolism (Brodersen et al., 2002; Liang et al., 2003; Lorrain et al., 2004; Tang et al., 2005), and autophagy (Liu et al., 2005).

To understand *RPW8* signaling, we examined the genetic interaction between *RPW8*-induced cell death and previously characterized defense response mutants and thereby established that salicylic acid (SA), and the SA pathway components *ENHANCED DISEASE SUSCEPTIBILITY1 (EDS1)*, *PHYTOALEXIN-DEFICIENT4 (PAD4)*, *EDS5*, and *NONEXPRESSOR OF PR1*, are required for *RPW8*-dependent HR and resistance (Xiao et al., 2003, 2005). These SA pathway components are not only activated by the *TIR-NB-LRR R* proteins for specific resistance but are also required for a basal level of resistance that operates even in susceptible hosts (Falk et al., 1999; Jirage et al., 1999; Nawrath et al., 2002). We also observed that the scale of the *RPW8*-triggered H₂O₂ accumulation and HR resulting from powdery mildew challenge was influenced by the genetic background and environmental conditions, with a varying number of cells involved in the HR at the fungal invasion site (Xiao et al., 1997, 2003). Furthermore, plants overexpressing *RPW8* from its native promoters exhibit spontaneous HR-like cell death (SHL) in the absence of any pathogens via a SA-dependent feedback amplification circuit (Xiao et al., 2003) that appears to be negatively regulated by *EDR1*, which encodes a mitogen-activated protein kinase kinase kinase implicated in defense signaling (Frye et al., 2001; Xiao et al., 2005). Hence, it is conceivable that the *RPW8*-triggered accumulation of H₂O₂ and HR is a double-edged sword that must be under tight control of both positive and negative regulation.

In order to further dissect the *RPW8* signaling pathway, we have conducted a genetic screen using T-DNA tagging for mutations that enhance *RPW8*-mediated HR-like cell death (designated *erh*). Here, we report the isolation and characterization of *erh1*, in which an *Arabidopsis* homolog (At2g37940) of animal sphingomyelin synthase (SMS) and protozoan inositolphosphorylceramide synthase (IPCS) is knocked out. We provide evidence that *ERH1* encodes an active plant IPCS and that loss of function of *ERH1* results in higher levels of ceramides in plants expressing *RPW8*. Ceramides are lipid molecules composed of a long-chain base and an amide-linked acyl chain. They serve as precursors to form more complex sphingolipids by the

addition of various sugar residues or phosphate-containing head groups to the ceramide moiety (Dunn et al., 2004). In yeast, protozoans, and plants, IPCS catalyzes the transfer of an inositol phosphate head group from phosphatidylinositol to ceramide, producing inositolphosphorylceramide (IPC) (Nagiec et al., 1997; Bromley et al., 2003; Denny et al., 2006). Ceramide derivatives not only provide structural integrity to eukaryotic cell membranes but also are believed to play important roles as second messengers in diverse cellular and physiological processes, such as cell differentiation and apoptosis in animals (Lei et al., 2007; Phan et al., 2007; Sanchez et al., 2007). Evidence is accumulating to suggest similar functions for sphingolipids in plants. For example, ceramide accumulation due to loss of function of *ACCELERATED CELL DEATH5 (ACD5)*, encoding a ceramide kinase, results in PCD in *Arabidopsis* (Liang et al., 2003). Results from this study provide evidence that sphingolipid (ceramide) metabolism plays an important regulatory role in plant PCD associated with *RPW8*-mediated broad-spectrum disease resistance.

RESULTS

Isolation and Phenotypic Characterization of *erh1*

Arabidopsis accession Col-0 lacks *RPW8* and is susceptible to powdery mildew (Xiao et al., 2001; Orgil et al., 2007). We selected a Col-0 line containing *RPW8* as a transgene (ST8) for mutagenesis. ST8 (the eighth generation of line S6 reported in Figure 1D of Xiao et al., 2003) contains two copies of *RPW8* under control of the native promoters and exhibits an intermediate level of SHL (Xiao et al., 2003). Thus, this line could be used to screen for mutations suppressing or enhancing *RPW8*-mediated SHL. In the screen for *erh* mutations (see Methods), we identified >20 putative *erh* mutants belonging to at least five complementation groups.

The first characterized *erh* mutant (*erh1*/ST8) was from a complementation group that contained two mutant lines from the same seed pool, and these two mutants were found to be derived from the same T1 individual by sequencing the genomic-T-DNA junctions. The *erh1*/ST8 mutant was backcrossed to ST8. All F1 plants had the same phenotype as ST8, indicating that the mutation was recessive. A total of 259 F2 plants grown in soil were scored for SHL and the presence of the T-DNA (reported by basta herbicide resistance). Of these, 26.6% (69 of 259) had the SHL phenotype seen in *erh1*/ST8, and these individuals were also all resistant to basta. These results suggested that a single T-DNA insertion in *erh1*/ST8 caused the enhanced SHL phenotype. A backcross (two generations)-purified *erh1*/ST8 mutant line was used for further characterization.

One week after seed germination in soil in short-day conditions (8 h of light, 16 h of dark; see Methods for plant growth conditions), very small lesions characteristic of SHL started to appear in *erh1*/ST8 cotyledons and true leaves and soon propagated to form big lesions that eventually engulfed the whole cotyledon/true leaf in a few days (Figure 1A). A close examination of the trypan blue-stained leaves showed that cell death first occurred in mesophyll cells around vascular tissues and then spread to neighboring cells, forming clusters of dead cells, which appeared as confined lesions to the naked eye (Figure 1A). Even

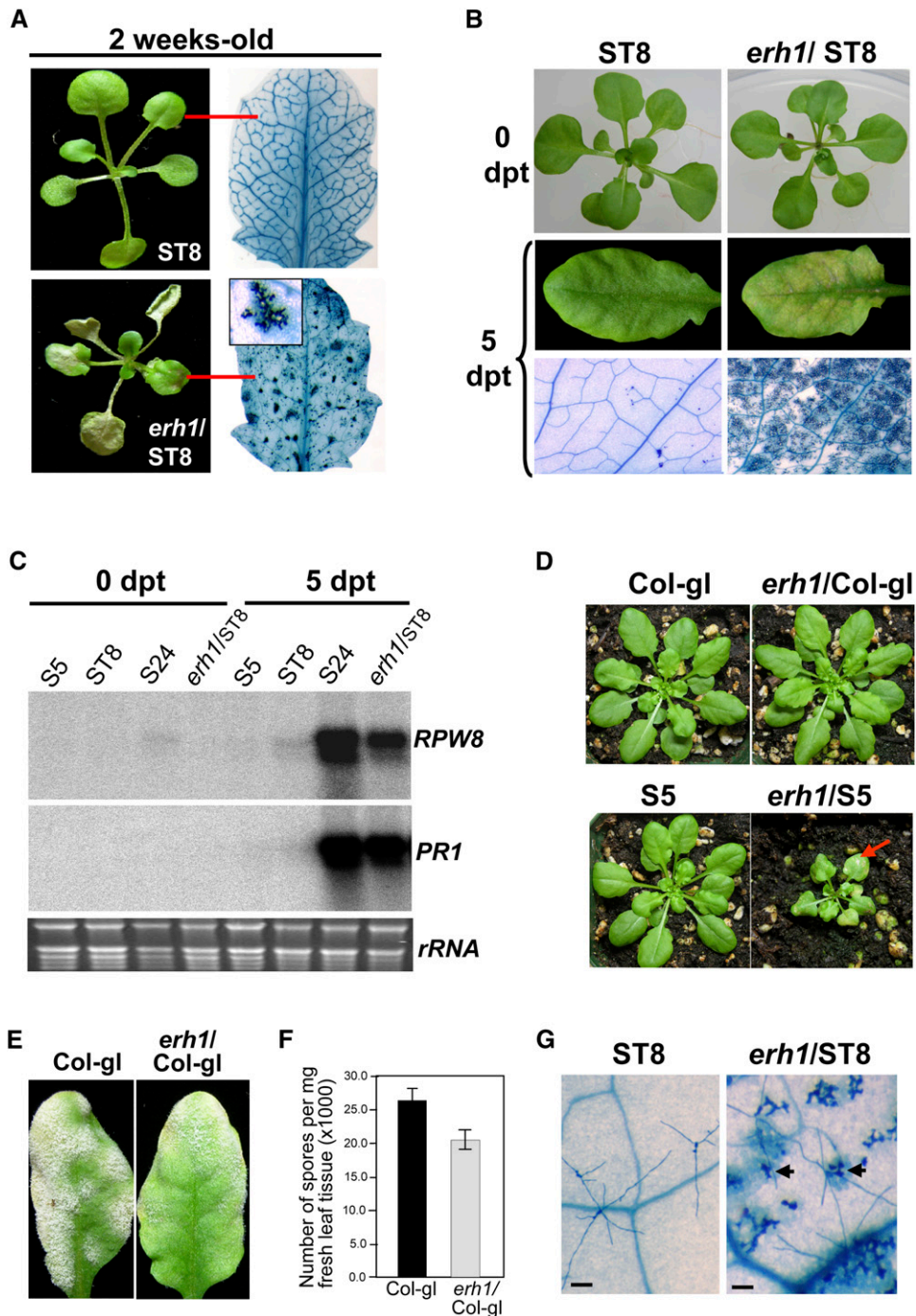


Figure 1. Isolation and Characterization of *erh1*.

(A) Soil-grown seedlings of the parental line (ST8) and the *erh1/ST8* mutant. A single representative leaf (indicated by red lines) stained with trypan blue is shown beside each seedling. The inset shows a cluster of dead cells at five times magnification.

(B) *erh1*-enhanced cell death is suppressed in plants grown on MS agar medium. Plants were grown in MS agar medium for 4 weeks and then transplanted into autoclaved soil. Photographs were taken at 0 or 5 d posttransplanting (dpt).

(C) *RPW8* expression is enhanced by *erh1*. Four-week-old plants of the indicated genotypes were transplanted from MS agar medium to autoclaved soil. Total RNA was extracted from fully expanded mature leaves at 0 or 5 dpt, gel-blotted, and probed with a ^{32}P -labeled cDNA mixture of *RPW8.1*, *RPW8.2*, and *PR1* sequentially. rRNA is shown as a loading control.

(D) *erh1*-induced cell death is largely *RPW8*-dependent. The *erh1* mutation from *erh1/ST8* was introduced into Col-gi and S5 (carrying a single copy of *RPW8*) by crossing. Photographs were taken at 5 weeks old. Note the SHL (indicated by the red arrow) and reduced stature of *erh1/S5*.

though massive SHL often kills most of the growing leaves, *erh1*/ST8 plants survived long enough to set seeds. However, the size of mutant plants was $\sim 1/10$ th that of the ST8 parental line at 5 weeks old. Interestingly, like *RPW8* overexpression-triggered SHL (Xiao et al., 2003), cell death in *erh1*/ST8 was also suppressed in plants grown on Murashige and Skoog (MS) agar medium (Figure 1B). However, when 6-week-old *erh1*/ST8 plants were transplanted from MS agar medium to autoclaved soil, massive SHL developed in mature and young leaves of *erh1*/ST8 plants in 5 to 7 d (Figure 1B). This response was comparable to the SHL seen in *RPW8* transgenic line S24, which contains at least four copies of *RPW8* and displays lethal SHL if grown in soil (Xiao et al., 2003). No visible cell death was observed in plants of the parental line ST8 at 10 d after transplanting (Figure 1B).

The T-DNA-induced mutation in *erh1*/ST8 was then crossed into Col-gi (Col-0 harboring the *glabrous* mutation), and an F3 individual that was homozygous for the *erh1* mutation and lacked *RPW8* was selected for phenotypic examination. Compared with Col-gi, *erh1*/Col-gi plants were normal in growth and development in the first 6 weeks in short-day conditions (8 h of light; Figure 1D). After 6 weeks, leaves of *erh1*/Col-gi plants gradually developed a few small chlorotic lesions visible to the naked eye, and trypan blue staining revealed sporadic cell death in *erh1*/Col-gi leaves (Figure 2B), indicating that *erh1* in the absence of *RPW8* results in a developmentally regulated mild cell death phenotype. To further confirm if *erh1* indeed enhances *RPW8*-triggered SHL, *erh1* was introduced from *erh1*/Col-gi into line S5, which harbors a single transgene containing *RPW8.1* and *RPW8.2* under control of their native promoters in Col-gi and does not exhibit SHL (Xiao et al., 2003). As expected, plants of *erh1*/S5 displayed strong SHL in soil-grown plants at 2 weeks after seed germination and had a reduced stature, reaching $\sim 30\%$ of the size of the parental S5 line at 5 weeks old (Figure 1D).

***erh1* Enhances *RPW8* Transcription and *RPW8*-Mediated HR via the SA Signaling Pathway**

To determine the mechanism by which *erh1* enhances *RPW8*-mediated cell death, we examined *RPW8* transcription and response to pathogens. To see if *RPW8* transcription is enhanced by *erh1*, we checked the expression of *RPW8* in the lines S5, ST8, *erh1*/ST8, and S24 at 0 and 5 d after transplanting from MS agar (SHL-suppressive conditions) to soil (SHL-permissive conditions). As we observed previously, *RPW8* expression in S24 plants increased dramatically (Figure 1C) (Xiao et al., 2003), due to the activation of a self-amplification circuit when *RPW8* reaches a threshold level under permissive conditions (e.g.,

soil). Amplification of *RPW8* expression correlated with strong induction of *PR1* (Figure 1C). We did not observe obvious induction of *RPW8* and *PR1* in S5 and ST8 plants after transplanting; however, we found that *RPW8* and *PR1* were highly induced in *erh1*/ST8 plants at 5 d after transplanting (Figure 1C). These results indicated that the *erh1* mutation enhances transcriptional amplification of *RPW8*, which in turn results in *PR1* expression and SHL.

To see if *erh1* alters the response to pathogens, we challenged 5-week-old plants of Col-gi, *erh1*/Col-gi, S5, and *erh1*/S5 with the powdery mildew isolate *Golovinomyces cichoracearum* UCSC1. *erh1*/Col-gi showed slightly reduced fungal mass on the leaf surface compared with wild-type Col-gi (Figure 1E). Quantification of susceptibility (see Methods) at 10 d postinoculation (dpi) showed that the number of spores per milligram of fresh leaf tissue in *erh1*/Col-gi was 76.5% of that in the wild type (Figure 1F), indicating that *erh1*/Col-gi is slightly, but significantly ($P < 0.05$), less susceptible than Col-gi. It was also noted that *erh1*/Col-gi leaves turned slightly pale at later development stages or after fungal infection.

Under regular infection conditions (Xiao et al., 2005), both S5 and *erh1*/S5 were resistant to *G. cichoracearum* UCSC1, making it difficult to assess if *erh1* enhances *RPW8*-mediated response to the pathogen. It has been shown that high humidity ($\sim 90\%$) attenuates *RPW8*-transcription and *RPW8*-triggered resistance to *G. cichoracearum* UCSC1 (Xiao et al., 2003). We thus grew S5, *erh1*/S5, ST8, and *erh1*/ST8 plants in MS agar medium for 5 weeks and then transplanted them into autoclaved soil and continued to grow them at 90% RH. Immediately after transplanting, plants were then inoculated with *G. cichoracearum* UCSC1. Two days later, inoculated leaves were stained with trypan blue to visualize the cell death and the fungal infection structures. We found that *RPW8*-mediated HR in response to *G. cichoracearum* UCSC1 was attenuated in S5 and ST8 under these conditions (Figure 1G), consistent with our previous observation (Xiao et al., 2003). By contrast, in inoculated leaves of *erh1*/S5 and *erh1*/ST8, fungal penetration in most cases was found to be associated with host cell death (HR), even though cell death not apparently associated with the fungus was also seen (Figure 1G). No or very little SHL was observed in uninoculated leaves of *erh1*/S5 and *erh1*/ST8 over the same time period. This observation indicated that the *erh1* mutation in the *RPW8* background triggered a more sensitive HR in response to powdery mildew infection, similar to previous observations for *edr1* in the *RPW8* background (Xiao et al., 2005).

We also tested *erh1*/Col-gi and Col-gi with the virulent bacterial pathogen *Pseudomonas syringae* pv *maculicola* strain ES4326

Figure 1. (continued).

(E) *erh1* in Col-gi results in reduced susceptibility to powdery mildew. Five-week-old, soil-grown plants of Col-gi and *erh1*/Col-gi were inoculated with *G. cichoracearum* UCSC1. Representative infected leaves from the indicated genotypes at 10 dpi are shown.

(F) Infected leaves of six plants from each genotype used in **(E)** were subjected to quantitative measurement of disease susceptibility (see Methods for details) at 10 dpi. Data represent means \pm SE of three replicate experiments ($P < 0.05$ based on Student's *t* test).

(G) *erh1*/ST8 has more pronounced HR in response to powdery mildew infection. Five-week-old plants were transplanted from MS agar medium to autoclaved soil and maintained at $>90\%$ RH. Plants were inoculated with *G. cichoracearum* UCSC1 immediately after transplanting. At 2 dpi, inoculated leaves were stained with trypan blue. Arrows indicate cell death induced by the fungus. Bars = 100 μ m.

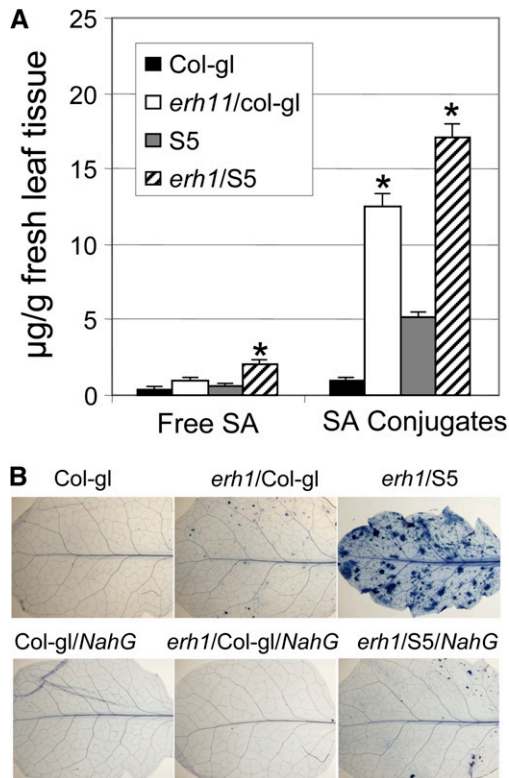


Figure 2. Involvement of SA in the *erh1*-Mediated Cell Death Phenotype.

(A) The *erh1* mutation results in SA accumulation. Leaves of 6-week-old plants of the indicated genotypes were assayed for free and total SA. The amount of conjugated SA is the subtraction of free SA from total SA. Data represent means \pm SE from three duplicate samples in one experiment. Asterisks indicate that the value of the *erh1* mutant is significantly different ($P < 0.01$) from that of the respective wild-type lines based on Student's *t* test. This experiment was repeated twice with similar results.

(B) *erh1*-activated SHL is SA-dependent. *erh1* and *erh1* plus *RPW8* (from line S5) were introduced into the *NahG* background by crossing, and respective F3 lines homozygous for *erh1* or *erh1/ RPW8* and *NahG* from the respective crosses were examined for SHL by trypan blue staining at 5 weeks old. [See online article for color version of this figure.]

and the congenic avirulent strain carrying *avrRpm1*, which elicits *RPM1* (a *CC-NB-LRR*-dependent HR and resistance (Grant et al., 1995). We did not find any significant difference in bacterial growth between Col-gl and *erh1/Col-gl* (see Supplemental Figure 1 online), suggesting that *ERH1* does not substantially contribute to defense against *P. syringae*.

To further investigate how the *erh1* mutation enhances *RPW8*-mediated cell death and the defense response, we measured the levels of SA in leaves of 6-week-old plants of Col-gl, *erh1/Col-gl*, S5, and *erh1/S5*. As shown in Figure 2A, compared with Col-gl, *erh1/Col-gl* had higher levels of free SA ($\sim 3\times$) and SA conjugates ($\sim 12.5\times$). Similarly, *erh1/S5* had higher SA levels ($3\times$ for both free SA and SA conjugates) compared with S5. Apparently, the *erh1* mutation resulted in increased SA accumulation independent of *RPW8*. Even though S5 accumulated 1.6 times the free SA and 5.2 times the conjugated SA compared with Col-gl,

erh1 in S5 resulted in a further accumulation of free SA and conjugated SA, with levels reaching 5.4 and 14.0 times those in Col-gl, respectively. These data indicate that the *erh1* mutation results in increased SA accumulation, possibly due to increased synthesis or decreased turnover, which in turn facilitates the SA-dependent feedback amplification of *RPW8* transcription, leading to SHL or HR and resistance.

To obtain further supporting evidence for this hypothesis, we individually introduced *NahG* and *pad4-1* into *erh1/Col-gl* and *erh1/S5* by crossing. It is known that *NahG* (a bacterial gene encoding a SA hydrolase) and *pad4-1* (a loss-of-function mutation of *PAD4*) suppress SA accumulation. We found that both *NahG* and *pad4-1* largely abolished *erh1*-triggered mild SHL in Col-gl or stronger SHL in S5 (Figure 2B), indicating that SA accumulation indeed contributes to *erh1*-triggered cell death.

Cloning of *ERH1*

We used inverse PCR (Does et al., 1991) to locate the insertion position of the T-DNA in *erh1/ST8*, and the results were confirmed by PCR with gene-specific primers (see Methods). Sequencing of the PCR products revealed that *erh1/ST8* had a T-DNA insertion in the third exon of *At2g37940* (Figure 3A), an expressed gene with unknown function. RT-PCR showed that *At2g37940* expression was completely knocked out in *erh1/ST8* (Figure 3B). Thus, *At2g37940* is the *ERH1* candidate gene.

Next, we cloned the genomic sequence of *At2g37940* and placed it under the control of the native promoter (~ 1.8 kb upstream of the ATG start codon) or the 35S promoter and introduced the corresponding DNA constructs into *erh1/S5* (Figure 3C). Expression of *At2g37940* from the native or the 35S promoter fully complemented the *erh1*-mediated SHL phenotype. We also made an RNA interference (RNAi) construct (cDNA of *At2g37940* in RNAi vector pJawohl8; Feys et al., 2005) to target *At2g37940* and introduced it into Col-gl and ST8. We found that 29% (18 of 62) and 34% (20 of 58) of transgenic lines displayed phenotypes similar to those seen in *erh1/Col-gl* and *erh1/ST8*, respectively. These genetic data clearly indicated that *At2g37940* is indeed *ERH1*.

ERH1 Shows Homology to Protozoan IPCS

Based on the annotation in the *Arabidopsis* database (<http://www.Arabidopsis.org>), *ERH1* (*At2g37940*) is predicted to contain 12 exons and 11 introns, with a coding sequence of 918 bp (Figure 3A). We sequenced the cDNA product from Col-0 and confirmed the predicted exon-intron structure. *ERH1* is predicted to encode a protein of 305 amino acids, with a molecular mass of 35 kD. The protein contains six transmembrane domains, which are predicted by TMpred (http://www.ch.embnet.org/software/TMPRED_form.html) and ConPred II (<http://bioinfo.si.hirosaki-u.ac.jp/~ConPred2/>) (Figure 3D), and has a weak phosphatidic acid phosphatase-related2 domain. *ERH1* has two homologs in the *Arabidopsis* genome, *At2g29525* and *At3g54020*, which respectively share 64 and 86% sequence identity with *ERH1* at the protein level. *At2g29525* and *At3g54020* were thus designated *ERH1-like1* (*ERHL1*) and *ERHL2*, respectively (see Supplemental Figure 2A online). A BLAST search identified

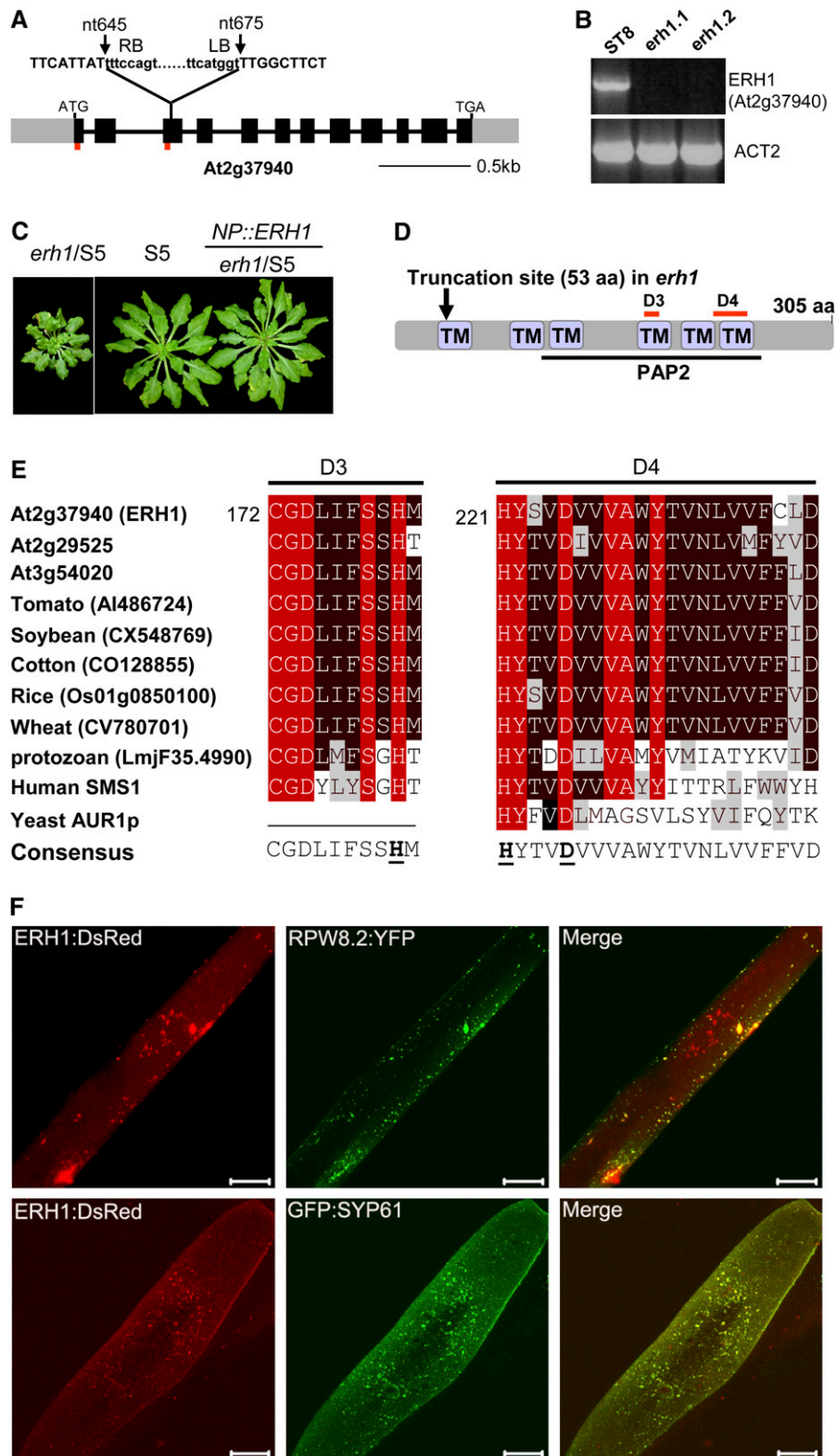


Figure 3. Cloning of *ERH1* and Subcellular Localization of the Protein.

(A) Schematic gene structure of *ERH1* (At2g37940) and the position of the T-DNA insertion. Two short red bars indicate the positions of the primers used for RT-PCR in (B).

numerous EST clones from various plant species showing 60 to 80% identity at the amino acid level to ERH1, suggesting that ERH1 and its homologs are highly conserved in plants.

The highest similarity to ERH1 identified outside the plant kingdom is to animal SMS (Huitema et al., 2004). For example, ERH1 shows 27% sequence identity and 44% similarity over a 148–amino acid stretch to human SMS1 (NP_671512; Hs SMS1). Similarity was also detected between ERH1 and the IPCS (LmjF35.4990; Lm IPCS) identified in a kinetoplastid protozoan (*Leishmania major*) (Denny et al., 2006). Although the amino acid sequence similarity in both cases is not high, the overall protein structures of ERH1, Hs SMS1, and Lm IPCS are very similar: all three are predicted to contain six transmembrane domains and a domain showing weak similarity to phosphatidic acid phosphatase-related2. Moreover, ERH1 and Lm IPCS show higher sequence similarity (~30 to 45% identity at the amino acid level) in the two domains designated D3 and D4 (Figures 3D and 3E), which are conserved between animal SMSs and the lipid phosphate phosphatase family (Waggoner et al., 1999). A BLAST search with the Hs SMS1 and Lm IPCS protein sequences also identified ERH1 and its two *Arabidopsis* homologs as the most similar sequences in the *Arabidopsis* genome. Collectively, these data suggest that ERH1 may be a functional homolog of protozoan IPCSs or animal SMSs.

SMSs in animals transfer the phosphorylcholine moiety from phosphatidylcholine onto the primary hydroxyl of ceramide, producing sphingomyelin and diacylglycerol (Ullman and Radin, 1974; Voelker and Kennedy, 1982; Marggraf and Kanfer, 1984; Huitema et al., 2004; Tafesse et al., 2007), whereas IPCSs in yeast and protozoa catalyze the production of inositolphosphorylceramide and diacylglycerol from ceramide and phosphatidylinositol (Nagiec et al., 1997; Denny et al., 2006) (see Supplemental Figure 2B online). We reasoned that ERH1 may be a functional homolog of Lm IPCS and yeast AUR1p, since plants have been known to synthesize phosphoinositol-containing sphingolipids and sphingomyelin has not been detected in yeast and plants (Carter et al., 1958; Kaul and Lester, 1975; Markham et al., 2006).

ERH1 Encodes an Active Plant IPCS

To test if *ERH1* indeed encodes an IPCS, we first asked if expression of *ERH1* in *Saccharomyces cerevisiae* could substitute for *AUR1*, an essential gene that encodes the sole IPCS (AUR1p) in yeast. The coding sequence of *ERH1* was cloned into the yeast vector pADH1-*LEU2*. This recombinant plasmid

(pERH1) was introduced into the yeast *aur1Δ* mutant that contained the yeast *AUR1* gene in the pRS316-*AUR1* plasmid. This plasmid rescues the lethal phenotype of *aur1Δ* and is *URA3*⁺-marked, enabling counterselection on fluoroorotic acid (FOA). Following transformation with pERH1, but not the pADH1 empty vector, the *aur1Δ* mutant was able to grow on medium containing FOA (Figure 4A), indicating that it was able to lose the pRS316-*AUR1* plasmid. This result demonstrates that ERH1 can substitute for AUR1p. We also found that expression of ERH1 could substitute for AUR1p in the *aur1Δ/scs7Δ* mutant, which lacks the ceramide-associated fatty acyl chain C2-hydroxylase (Haak et al., 1997) (Figure 4A), indicating that, like AUR1p, ERH1 can use non-C2-hydroxy ceramides as a substrate. Furthermore, we found that ERH1 could substitute for AUR1p in the *aur1Δ/sur2Δ* mutant, which lacks the sphinganine (d18:0, dihydro-sphingosine; DHS) C4-hydroxylase that catalyzes the formation of the major yeast long-chain base phytosphingosine (PHS; t18:0). These data indicate that ERH1 has a broad substrate specificity independent of the hydroxylation status of the ceramide (Figure 4A).

To gain direct biochemical evidence that ERH1 is an IPCS, we prepared microsomes from the *aur1Δ* mutant yeast harboring a plasmid expressing yeast *AUR1* (pAUR1) or *ERH1* (pERH1) and analyzed the IPCS activity using PHS-, DHS-, and sphingosine-containing 12-(*N*-methyl-*N*-(7-nitrobenz-2-oxa-1,3-diazol-4-yl)) (NBD) C6-ceramides. As shown in Figure 4B, microsomes from ERH1-expressing yeast cells transferred inositolphosphate to ceramides containing either DHS or PHS, albeit at a lower efficiency compared with that from AUR1p-expressing cells. However, the IPCS activity of the ERH1-containing microsomes toward sphingosine-containing ceramide was very weak, as indicated by the barely detectable band of the IPC product (Figure 4B).

To confirm that ERH1 is an active plant IPCS, total protein extracts were prepared from leaves of 6- to 8-week-old S5 and *erh1/S5* plants (see Methods). The extracts were then coincubated with soy phosphatidylinositol and dodecanoyl-NBD-D-*erythro*-DHS as substrates, and the IPCS activities were measured by quantification of the fluorescent IPC product. We chose dodecanoyl-NBD-D-*erythro*-DHS as a substrate because NBD-ceramide having DHS as the long-chain base appeared to be a better substrate than NBD-ceramide having sphingosine in our yeast assays (Figure 4B). As shown in Figure 4C, compared with S5 (100%), *erh1/S5* showed reduced IPCS activity (53.3%), indicating that ERH1 accounts for about half of the total IPCS

Figure 3. (continued).

(B) RT-PCR with the parental line and two *erh1/ST8* siblings for *ERH1* and *ACT2*.

(C) Genetic complementation of *erh1* with *ERH1* under the control of the native promoter (*NP*).

(D) Predicted protein structure of ERH1. PAP2, phosphatidic acid phosphatase-related2; TM, transmembrane. D3 and D4 are two conserved domains found in functional homologs.

(E) Alignment of two conserved motifs, D3 and D4, from predicted plant ERH1-like protein sequences, a kinetoplastid (*L. major*) IPCS, human SMS1, and yeast (*Saccharomyces cerevisiae*) AUR1p. Identical residues are highlighted in red, and conservative residues are highlighted in black or gray. Underlined in the consensus are three residues that form a catalytic triad required for enzymatic function (Huitema et al., 2004).

(F) Subcellular localization of ERH1. Plasmid DNA of 35S:*ERH1-DsRed* was mixed in equal amounts with that of *NP:RPW8.2-YFP* or 35S:*GFP-SYP61* (a *cis*-Golgi marker) or other constructs (see Supplemental Figure 4C online) and introduced into Col-0 leaf epidermal cells by bombardment (see Methods). Expression of the fluorescence-tagged proteins was imaged with a laser confocal microscope at 24 h after bombardment. Bars = 10 μm.

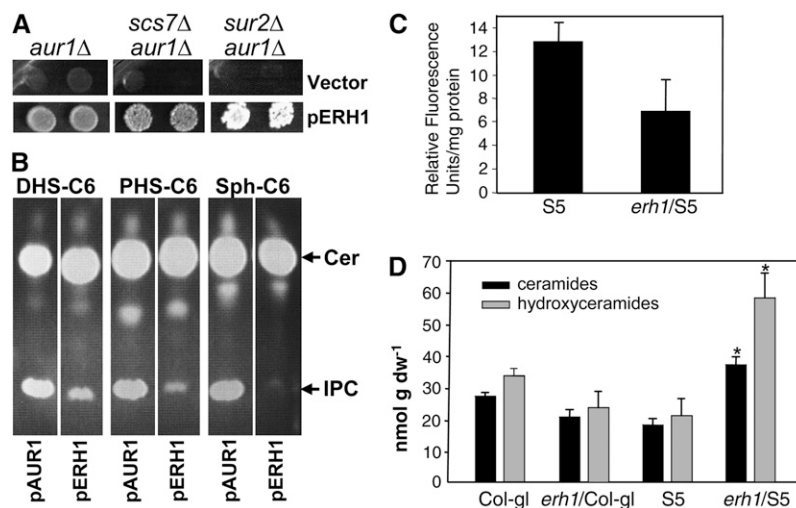


Figure 4. *ERH1* Encodes an IPCS.

(A) Complementation of the yeast *aur1* mutation by *ERH1*. *ERH1* was cloned in the pADH-LEU2 plasmid. The parental and the recombinant plasmids were introduced into three yeast strains lacking AUR1p alone (*aur1Δ*), AUR1p and ceramide-associated fatty acyl chain C2-hydroxylase (*aur1Δ/scs7Δ*), or AUR1p along with sphinganine hydroxylase (*aur1Δ/sur2Δ*). The respective yeast cells were grown on SD medium (–Leu) containing FOA.

(B) Yeast cells expressing *ERH1* possess IPCS activities. Microsomes were prepared from *aur1Δ* yeast cells harboring pAUR1 or pERH1 and assayed for IPCS activities using the indicated ceramide substrates. Note that IPCS activities are reflected by the production of IPC (bottom bands) from the ceramide substrate (strong top bands). Cer, ceramide; Sph, sphingosine.

(C) In vitro assays for plant IPCS activity. Leaf lysates were prepared from 6-week-old plants and subjected to IPCS assays using dodecanoyl-NBD-D-erythro-DHS as a substrate. IPCS activity was measured using relative fluorescence units. Data are means \pm SE ($P < 0.015$ based on Student's *t* test of the values of the two genotypes; $n = 4$).

(D) *erh1* results in ceramide accumulation in plants expressing *RPW8*. Sphingolipids were extracted from leaves of 8-week-old plants of the indicated genotypes and measured essentially as described previously (Markham and Jaworski, 2007). Values are means \pm SE ($n = 5$). Asterisks indicate significance at $P < 0.01$ compared with S5 based on Student's *t* test. dw, dry weight.

activity in mature leaf tissue. The partial reduction in the IPCS activities in *erh1/S5* is not unexpected, since the *Arabidopsis* genome contains two *ERH1* homologs (see Supplemental Figure 2A online).

Given the biochemical function of *ERH1* as a plant IPCS, one would predict that loss of function of *ERH1* may result in the accumulation of ceramides and/or reduced levels of IPC or more complex glycosylated IPCs. To test this, we measured total sphingolipids from leaves of 6-week-old plants of Col-gl, *erh1/Col-gl*, S5, and *erh1/S5*. Comparative analyses of the sphingolipid profiles revealed that the total amounts of ceramides and hydroxyceramides in *erh1/S5* were significantly higher ($P < 0.01$) than those in the other three genotypes (Figure 4D) and that there were no significant differences in other sphingolipids (see Supplemental Figures 3A to 3E online). Significant accumulation of ceramides in *erh1/S5* but not in *erh1/Col-gl* correlated with higher levels of SA and much more spontaneous cell death in the former and thus implies a synergistic relationship between *RPW8* expression, SA and ceramide accumulation, and PCD.

***ERH1* Is Largely Localized to the *trans*-Golgi Network**

To test if *ERH1* is also expressed in other organs and tissues apart from leaves, we checked the expression pattern of *ERH1* by RT-PCR and found that it was expressed in all organs and tissues examined (see Supplemental Figure 4A online). Ceramide

is synthesized at the endoplasmic reticulum and translocated to the Golgi compartment for conversion to more complex sphingolipids (Hanada et al., 2003). Consistent with this, yeast AUR1p and human SMS1 are found to be located to the Golgi apparatus (Levine et al., 2000; Tafesse et al., 2007). We thus asked if *ERH1* also resides in the Golgi compartment. For this, we made a fusion construct under the control of the 35S promoter such that *ERH1* is fused with yellow fluorescent protein (YFP) at its C terminus. We first introduced the construct into *erh1/S5* and found that it rescued the SHL phenotype, indicating that the fusion protein is functional. However, confocal examination of the leaves of *erh1/S5* or Col-0 plants transgenic for 35S:*ERH1*-YFP could not detect obvious fluorescence, implying that the protein expression level is very low. We thus took a transient expression approach to determine its likely subcellular localization. Transient overexpression of 35S:*ERH1*-YFP in onion (*Allium cepa*) epidermal cells gave a punctate distribution of YFP fluorescence (see Supplemental Figure 4B online), suggesting a likely endomembrane localization. To find the specific cellular compartment(s) in which *ERH1* is localized, we made the 35S:*ERH1*-DsRed construct and bombarded leaves of Col-0 with the plasmid DNA of either 35S:*ERH1*-YFP or 35S:*ERH1*-DsRed, with plasmids containing 35S:*mCherry*-AtWAK2-HEDL (Nelson et al., 2007), 35S:*ERD2*-GFP (daSilva et al., 2004), and 35S:*GFP*-SYP42 and 35S:*GFP*-SYP61 (Sanderfoot et al., 2001; Uemura et al., 2004) producing marker proteins for the endoplasmic reticulum, the

Golgi bodies, and the *trans*-Golgi network, respectively. ERH1: DsRed did not show obvious colocalization with mCherry: AtWAK2:HEDL or ERD2:GFP; however, it did colocalize with GFP:SYP42 and GFP:SYP61, indicating that ERH1 is localized to the *trans*-Golgi network (Figure 3F; see Supplemental Figure 4C online). We also biolistically introduced plasmids expressing RPW8.2:YFP and ERH1:DsRed into Col-0 epidermal cells. Interestingly, ERH1 and RPW8.2 showed overlapping localization (Figure 3F).

ERH1 Is Upregulated in the RPW8 Overexpression Background and during HR

As ERH1 has been defined as a putative negative regulator of RPW8 signaling (Figure 1), we reasoned that ERH1 may be expressed at higher levels in the RPW8 background in order to curb RPW8-triggered HR or SHL. To test this idea, we measured the ERH1 mRNA levels in leaves of 6-week-old soil-grown Col-gi, S5, and ST8 plants and in leaves of S24 plants grown on MS agar medium (no cell death) for 5 weeks and then transplanted into soil for 5 d (cell death initiated). We found that the ERH1 mRNA levels in ST8 and S24 were 2.7 and 7.3 times that in Col-gi, while there was no significant difference between S5 and Col-gi (Figure 5A). This pattern of ERH1 expression correlates with the higher copy number of RPW8 in lines S5, ST8, and S24 (one, two, and four, respectively) and the degree of RPW8-triggered SHL phenotypes (none, mild, and severe, respectively), suggesting that the function of ERH1 is mechanistically associated with RPW8-mediated cell death.

To examine if expression of ERH1 correlates with defense signaling, we asked whether exogenous SA application can induce ERH1. We sprayed Col-0 plants with 0.5 mM SA or water and measured the ERH1 mRNA levels by quantitative RT-PCR at 24 and 48 h after treatment. There was no significant change (<1.5 fold) before and after SA or water treatment (see Supplemental Figure 5 online). To see if ERH1 expression correlates with HR activation, we measured the ERH1 mRNA levels in Col-0 and S5 prior to inoculation and at 3 or 5 dpi with powdery mildew. As shown in Figure 5B, we found that ERH1 was slightly but significantly induced in Col-gi by powdery mildew inoculation at 5 dpi (2.2×). By contrast, ERH1 was more strongly (4.4×) induced at 3 dpi in S5, and the level dropped slightly (3.5×) at 5 dpi compared with Col-gi or S5 without infection. The higher ERH1 expression at 3 dpi in S5 coincided with the onset of HR activated by RPW8 in response to fungal invasion (Xiao et al., 2005).

Next, we examined ERH1 expression in response to inoculation with a virulent or an avirulent bacterial pathogen. Six-week-old Col-0 wild-type plants were inoculated with the virulent *P. syringae* pv *maculicola* strain ES4326 or the congenic avirulent strain carrying *avrRpm1*, which elicits RPM1-dependent HR and resistance (Grant et al., 1995). ERH1 was expressed at a very low level in unchallenged leaves and was barely induced by inoculation of the virulent strain (Figure 5C). By contrast, ERH1 was rapidly induced by the avirulent strain as early as 0.5 h after inoculation before the onset of HR. The induction of ERH1 peaked at 4 to 8 h after inoculation before the defense marker gene *PR1* was highly induced (Figure 5D).

Combined, these results indicated that ERH1 is specifically associated with RPW8-triggered SHL and defense-associated HR.

erh1 and acd5 Activate Cell Death Additively or Synergistically

It was reported that *acd5*, a loss-of-function mutation in *ACD5* encoding a ceramide kinase, results in ceramide accumulation and developmentally regulated cell death (Liang et al., 2003). To test if ceramide accumulation is indeed associated with SHL and enhanced defense responses in *erh1/S5* plants, we first inoculated 5-week-old *acd5* plants before development of cell death lesions with *G. cichoracearum* UCSC1 and found that, compared with Col-0, *acd5* had clear enhanced resistance to the pathogen (Figure 6A), which is more obvious than that seen in *erh1/Col-gi* (Figure 1E).

Next, we introduced *acd5* into the S5 background to see if it could enhance RPW8-triggered SHL. Compared with *acd5*, which did not develop cell death until ~6 weeks old under our growth conditions (8 h of light, ~80% RH), *acd5/S5* developed necrotic cell death lesions at ~4 weeks old and had slightly reduced plant stature (Figure 6B). Cell death of *acd5/S5* also became more severe at later developmental stages compared with that of *acd5*.

We then made the *erh1/acd5* double mutant and found that, compared with the single mutants, the double mutant plants developed earlier (at ~4 weeks old) and more severe necrotic lesions (Figure 6C).

Finally, we introduced these two mutations into S5 by crossing and found that the *erh1/acd5/S5* plants developed very strong cell death on cotyledons and true leaves at 1 week after seed germination in soil (Figure 6D) but managed to set seeds when grown in MS agar and then in soil despite greatly reduced plant stature.

These results suggest that there is an apparent additive or synergistic effect between *acd5*- and *erh1*-mediated cell death in leaf tissues and that ceramide accumulation in *erh1* may account for accelerated cell death activation in the RPW8 background.

Downregulation of the Rice Homolog of ERH1 Leads to SHL and Reduced Plant Stature

To see if the function of ERH1-like genes is conserved in crop species, we generated rice (*Oryza sativa*) transgenic lines carrying an RNAi construct targeting the probable ortholog of rice ERH1 (Os01g0850100; designated Os ERH1). Among four transgenic lines analyzed, two showed obvious SHL and reduced plant stature (~70% of the wild-type level) (Figure 6E). RT-PCR showed that only these two lines (lines 46 and 51) with SHL had reduced mRNA levels of Os ERH1 (Figure 6F). This result suggests a likely conserved function in the control of PCD for ERH1-like genes across plant species.

DISCUSSION

By taking a genetic approach, we have identified *At2g37940* (*ERH1*) as a potential negative regulator of RPW8-mediated cell death associated with defense activation. Sequence homology

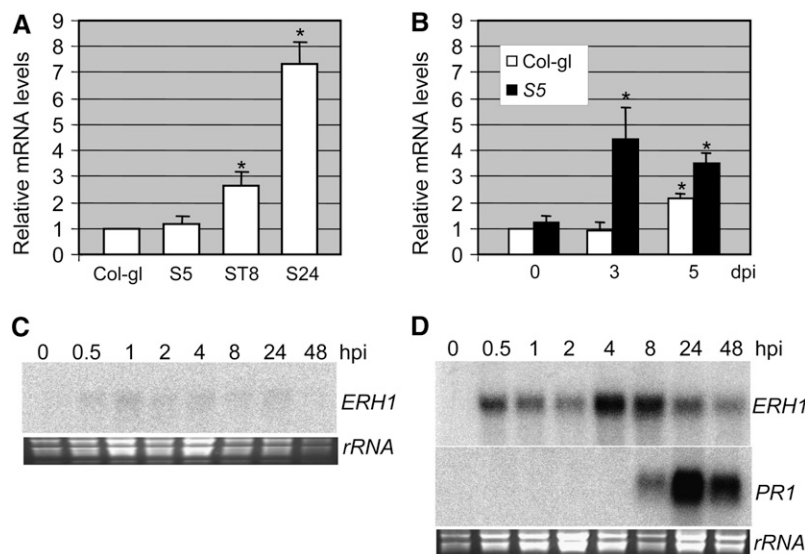


Figure 5. Induction of *ERH1*.

(A) *RPW8* overexpression leads to enhanced *ERH1* expression. Expression levels of *ERH1* in 6-week-old plants (except S24, which was grown in MS agar for 5 weeks and transplanted to soil for 5 d) were measured by quantitative RT-PCR using TaqMan chemistry. The relative mRNA levels in *RPW8*-expressing lines were calculated relative to that of Col-gl (1.0). Data represent means \pm SE from three replicate experiments. Asterisks indicate significance at $P < 0.01$ compared with Col-gl based on Student's *t* test.

(B) *ERH1* is induced to higher levels by powdery mildew. Six-week-old plants were inoculated with *G. cichoracearum* UCSC1. cDNA was synthesized from mRNA extracted from leaf tissues of the indicated genotypes at 0, 3, or 5 dpi and used for transcript quantification by real-time RT-PCR. The relative mRNA levels were calculated relative to that of Col-gl at 0 dpi (1.0). Data represent means \pm SE from three replicate experiments. Asterisks indicate significance at $P < 0.01$ compared with Col-gl based on Student's *t* test.

(C) and **(D)** *ERH1* is induced by avirulent *P. syringae*. Total RNA was extracted from leaves of 6-week-old Col-0 plants infiltrated with the virulent *P. syringae* pv *maculicola* ES4326 strain ($OD_{600} = 0.0002$) **(C)** or the avirulent strain carrying *AvrRpm1* **(D)** at the indicated time points, gel-blotted, and probed with ^{32}P -labeled *ERH1* or *PR1* cDNA. hpi, hours postinoculation.

analysis suggested that *ERH1* may be the long-sought functional homolog of protozoan and yeast IPCSs that convert ceramide to IPC. Indeed, we found that *ERH1* could complement the yeast *IPCS* (*aur1*) mutation and that expression of *ERH1* in *aur1* Δ yeast cells and loss of function of *ERH1* in *Arabidopsis* plants accounted for the complemented and reduced IPCS activities in the respective organisms (Figures 4B and 4C). Thus, our work has led to the identification of a plant IPCS gene and provided evidence for a critical role of sphingolipid metabolism in the regulation of plant PCD associated with pathogen resistance.

Sphingolipids are known to function in all eukaryotic cells as membrane structural components and as bioactive molecules involved in signal transduction and cell regulation (Dunn et al., 2004; Lynch and Dunn, 2004). Numerous reports have shown that sphingolipids such as ceramide play essential regulatory roles in the induction of animal apoptosis (Lei et al., 2007; Phan et al., 2007; Sanchez et al., 2007). The aberrant cell death in each of the two *Arabidopsis* mutants (*acd11* and *acd5*) was most likely caused by perturbation of sphingolipid metabolism, which is supported by the in vitro enzymatic activities of *ACD11* and *ACD5* as a sphingosine transfer protein and a ceramide kinase, respectively (Brodersen et al., 2002; Liang et al., 2003). These parallel emerging pictures for the role of sphingolipids in cell death regulation, from both the plant and animal kingdoms, suggest that there may be a common, fundamental mechanism

of cell fate regulation by sphingolipids. This speculation is supported by the findings that mycotoxins such as fumonisin and AAL (*Alternaria alternata* f. sp. *lycopersici*) toxin, which disrupt sphingolipid metabolism by inhibiting sphinganine *N*-acyltransferase, promote cell death in both animals (Wang et al., 1996b; Desai et al., 2002) and plants (Wang et al., 1996a).

Given that *ERH1* is homologous to animal SMSs that convert ceramide to sphingomyelin, the predominant sphingolipid in mammals (Hakomori, 1983), and that inhibition of SMS activities induces apoptosis (Meng et al., 2004; Ding et al., 2008), our finding that *erh1* enhances *RPW8*-dependent cell death and resistance to powdery mildew in *Arabidopsis* further augments the notion that there may be a common mechanism in cell death regulation or execution in both plants and animals.

However, sphingomyelin has not been detected in plants (Dunn et al., 2004), posing a question regarding what biochemical function *ERH1* may have in plants. Like plants and yeast, the kinetoplastid protozoa synthesize IPC rather than sphingomyelin. By utilizing bioinformatic and functional genetic approaches, Denny et al. (2006) isolated a functional ortholog of *AUR1* (LmjF35.4990) in the kinetoplastids (*L. major*) and demonstrated that it possessed IPCS-like activity when expressed in mammalian cells. Interestingly, like *ERH1*, the protozoan IPCS shows higher homology to animal SMSs than to yeast *AUR1p*. Thus, it was not a surprise to us that our genetic and biochemical assays

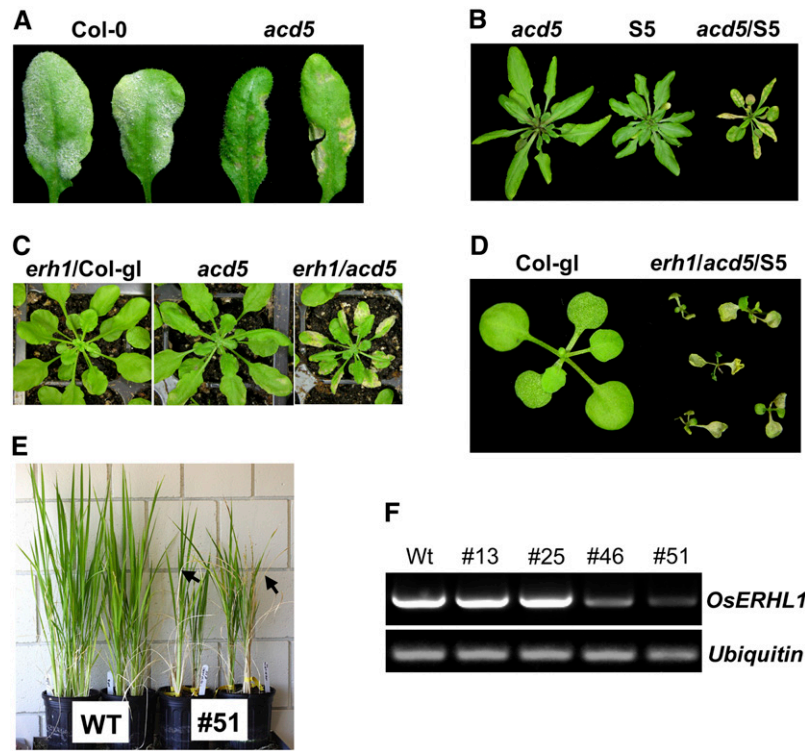


Figure 6. Additive/Synergistic Effects of *acd5* and *erh1* on Cell Death.

- (A) *acd5* has enhanced resistance to powdery mildew. Five-week-old plants were inoculated with *G. cichoracearum* UCSC1, and disease phenotypes at 8 dpi were shown by two representative leaves for each genotype. Powdery mildew infection can be seen as white powdery coating on Col-0 leaves.
- (B) Six-week-old, short-day-grown plants of the indicated genotypes. Note the leaf cell death and reduced plant stature of *acd5/S5*.
- (C) Four-week-old, short-day-grown plants of the indicated genotypes. Note the leaf cell death and reduced plant stature of *erh1/acd5*.
- (D) Two-week-old, short-day-grown plants of the indicated genotypes. Note the collapsed cotyledons and stunted growth of *erh1/acd5/S5*.
- (E) Silencing a rice *ERH1* homolog leads to cell death and reduced plant stature. Two-and-one-half-months-old wild-type Nipponbare rice and one representative rice line transgenic for an RNAi construct targeting a rice *ERH1* homolog (Os01g0850100) are shown. Arrows indicate dead leaves.
- (F) RT-PCR analysis of the indicated genes from four rice transgenic lines along with the parental wild type.

demonstrated that *ERH1* indeed encodes an active plant IPCS (Figures 4A to 4C). It is worth noting that the sequence motif H-[YFWH]-X2-D-[VLI]-X2-[GA]-X3-[GSTA], which is shared by previously characterized lipid phosphate phosphatase family members and AUR1p homologs in fungi (Waggoner et al., 1999), is also conserved in animal SMSs, Lm IPCS, and ERH1 (defined as the D4 domain in Huitema et al., 2004) (Figure 3E), and the His and Asp residues (underlined) that are assumed to be required for catalytic activity (Neuwal, 1997) are absolutely conserved in all of these homologs (Figure 3E).

The identification of ERH1 as a plant IPCS supports the notion that biochemically there exists a divergence at an early step of ceramide metabolism among kingdoms: while ceramide is converted to sphingomyelin in animals, it is converted to IPC in fungi, kinetoplastids, and plants (see Supplemental Figure 2B online) (Denny and Smith, 2004). However, because both the plant (e.g., ERH1) and the protozoan (e.g., Lm IPCS) functional homologs of yeast AUR1p show higher homology to animal SMSs than to yeast AUR1p, it seems likely that the dichotomic split with regard to sphingolipid biosynthesis might have occurred more than once. Phylogenetic analysis of animal SMSs and yeast, proto-

zoan, and plant IPCSs suggests that at least three evolutionary splits might have occurred concerning the initial step of ceramide metabolism (see Supplemental Figure 2C and Supplemental Data Set 1 online).

Based on the biochemical function of ERH1 (i.e., as a plant IPCS), loss of function of *ERH1* is expected to cause two direct consequences: accumulation of ceramide and reduction of IPC or its more readily detectable glycosylated derivatives (GIPCs). Our sphingolipid profiling results showed that there were significant increases ($P < 0.01$) of ceramide and hydroxylceramide levels in *erh1/S5* compared with those in S5. Interestingly, the increase in ceramides appeared to be as t18:0 (PHS)-containing ceramide species, of which a significant amount was t18:0 c16:0 (palmitic acid) (Figure 4D). No significant differences were detected in the levels of GIPCs, glucosylceramides, sphingoid long-chain bases, and their phosphorylated derivatives (see Supplemental Figures 3A to 3E online). It is possible that levels of GIPCs may have been maintained in *erh1/S5* through some compensatory mechanisms, although, given the higher amounts of GIPCs present in plants, any depletion in GIPC levels may have been too small to detect. Elevated levels of ceramides and

hydroxyceramides in *erh1/S5* are consistent with the hypothesis that ceramide plays an important role in the activation of *RPW8*-dependent cell death. Additional evidence supporting this came from our genetic and phenotypic analyses of *acd5* in combination with *erh1* and *RPW8*. We found that *acd5* plants, which have elevated levels of ceramides (Liang et al., 2003), showed enhanced resistance to powdery mildew and also exhibited exacerbated cell death in the S5 (*RPW8*) background (Figures 6A and 6B). Moreover, the *acd5/erh1* double mutant developed an earlier and much stronger cell death phenotype in both the Col-0 and S5 backgrounds (Figures 6C and 6D). It was recently reported that loss of function of *EDR2* causes enhanced resistance to powdery mildew in *Arabidopsis* and that the inhibition of fungal growth coincides with pathogen-induced host cell death (Tang et al., 2005; Vorwerk et al., 2007). *EDR2* encodes a novel protein that contains a pleckstrin homology domain and a steroidogenic acute regulatory protein-related lipid-transfer domain, both found in the human ceramide transport protein CERT (Hanada et al., 2003). It is thus possible that *edr2*-mediated enhanced powdery mildew resistance may be attributed to perturbation of ceramide metabolism.

Cell death in *erh1/S5* appears to be influenced by environmental conditions. Similar to the observation we made previously with S24 (Xiao et al., 2003), SHL was suppressed in *erh1/S5* plants grown on MS agar plates, even though other growth conditions (i.e., light, temperature, and RH) were similar or identical. How MS agar medium conditions inhibit SHL development remains to be determined. Cell death in *erh1/S5* also appears to be developmentally regulated. SHL became visible in true leaves of 2-week-old seedlings of *erh1/S5*, and the plant stature was permanently reduced. By contrast, *acd5/S5* plants appeared to have normal growth and development in the first 4 weeks, reaching a similar rosette size as S5, and then developed big necrotic lesions that in some cases propagated to engulf the whole leaf. Despite an earlier occurrence and a more severe phenotype, the pattern of cell death in *acd5/S5* is similar to that observed in *acd5/Col-0* (Greenberg et al., 2000) but different from that in *erh1/S5* (Figures 1 and 6). These observations suggested that *ERH1* and *ACD5* may fulfill different but essential biological functions in different or perhaps overlapping developmental stages.

HR cell death is often, although not always, associated with resistance against biotrophic pathogens such as powdery mildew and, to a lesser degree, with resistance against hemibiotrophic pathogens such as *P. syringae*. It is conceivable that HR cell death must be tightly regulated in plants to avoid unnecessary host cell death at the site of pathogen infection. Therefore, *ERH1* may function to curb *RPW8*-dependent cell death. Consistent with this idea, we found that *ERH1* induction occurred before or coincided with the onset of HR cell death, and there was no apparent or only a slight induction of *ERH1* during compatible interactions with bacterial and fungal pathogens (Figures 5B and 5C). Mining of gene expression data in the National Center for Biotechnology Information database also found that *ERH1* was induced to higher levels by powdery mildew (Nishimura et al., 2003; Stein et al., 2006) and by necrosis- and ethylene-inducing peptide extracted from *Fusarium oxysporum* (Bae et al., 2006). It remains unclear what role increased expression of *ERH1* has

during pathogen infection, but it presumably serves to increase GIPC biosynthesis for a defense-related function.

How *erh1*- and *acd5*-caused ceramide accumulation enhances *RPW8*-dependent cell death is not clear. In animals, ceramide accumulation has been known to induce apoptosis via multiple pathways (Pettus et al., 2002). Given that *RPW8*-triggered SHL, HR, and resistance involve an SA-dependent feedback amplification circuit, one likely scenario is that disruption of *ERH1* or *ACD5* somehow results in SA accumulation, which further strengthens *RPW8* signaling, resulting in cell death. Indeed, the *erh1* mutation in Col-g1 and S5 resulted in 3 to 12 times increases of free SA and SA conjugates (Figure 2A), supporting this speculation. Similarly, the SA level in *acd5* mutant plants also had an approximately fivefold increase compared with the wild type (Greenberg et al., 2000). Furthermore, depleting SA by the expression of *NahG* or blocking the SA signaling pathway by *pad4-1* (in *erh1*; Figure 2B) and *eds5-1* (in *acd5*; Greenberg et al., 2000) abolished the cell death phenotype caused by *erh1* and *acd5*, respectively. These observations collectively suggest that normal sphingolipid metabolism is probably important for SA homeostasis required for cell survival and that ceramide accumulation may cause overproduction and accumulation of SA via an unknown mechanism, leading to PCD associated with defense signaling. Because *erh1/S5* but not *erh1/Col-g1* showed accumulation of ceramides, we reason that *RPW8*'s function must be somehow affected by *erh1*, which results in further SA accumulation in plants expressing *RPW8*, leading to ceramide accumulation, thus explaining *erh1*-triggered, *RPW8*-dependent cell death.

In spite of cell death and the activation of defense-related genes (i.e., *PR1*), *acd5* did not show resistance to a virulent bacterial pathogen, *P. syringae*, leading to the conclusion that SA-dependent cell death and defense gene expression are uncoupled in *acd5* and that the cell death in *acd5* may mimic disease-caused cell death in plants (Greenberg et al., 2000). In this study, we also found that *erh1/Col-g1* was as susceptible as the wild type to a virulent *P. syringae* strain. However, both *erh1/Col-g1* and *acd5/Col-0* had enhanced resistance to powdery mildew. This pattern of defense is consistent with our earlier observation that *RPW8*-activated defense signaling does not contribute to resistance to *P. syringae*; instead, *RPW8* overexpression results in slightly enhanced susceptibility to this bacterial pathogen (Wang et al., 2007). Combined, these results suggest that subtle differences exist in the efficacy of SA signaling and HR cell death in resistance against biotrophic pathogens (such as powdery mildew) and hemibiotrophic pathogens (such as *P. syringae*) and that cell death and SA signaling activated by *acd5* and *erh1* appear to be effective only against biotrophic pathogens. One likely explanation for this phenomenon is that biotrophic pathogens such as powdery mildew strictly require living cells to establish infection and complete their life cycle, and cell death caused by ceramide accumulation may pose a physical barrier for the pathogen to grow and thrive. However, for hemibiotrophic bacterial pathogens such as *P. syringae*, once they are delivered into host tissues by injection, their multiplication is much faster and may not be affected by cell death caused by ceramide accumulation, even if it is accompanied by the activation of SA signaling.

There are two SMS homologs in the human genome. SMS1 functions in the Golgi, while SMS2 works at the plasma membrane (Tafesse et al., 2007). ERH1 is mainly localized to the *trans*-Golgi network (Figure 3F). The subcellular localization and function of the two *Arabidopsis* homologs of ERH1 remain to be determined. Functional redundancy between ERH1 and its homologs is likely, which could explain why *erh1*-triggered cell death is weaker in the Col-gi background compared with that caused by loss of function of the single-copy ceramide kinase gene (Liang et al., 2003). Construction and characterization of double and triple mutants for *ERH1* and its homologs should clarify these questions.

There is indirect evidence for the involvement of *ERH1*-homologous genes (based on EST clones) in pathogen defense in other plant species. For example, a rice *ERH1* homolog (Os05g0287800) was found to be induced by an avirulent pathogen (N1141 strain of *Acidovorax avenae*) (Fujiwara et al., 2004), and a soybean (*Glycine max*) *ERH1* homolog (CD411105) was slightly induced by SA and *Phytophthora sojae*, race 1 (Tian et al., 2004). In this study, we have demonstrated that a rice *ERH1* homolog (Os01g0850100) also appeared to function as a negative regulator of PCD in rice (Figure 6E), providing genetic evidence for likely functional conservation of *ERH1*-like genes across plant species. This functional conservation may provide a potential new avenue for enhancing disease resistance of crop species against biotrophic pathogens by targeted downregulation of the corresponding *ERH1*-like genes using pathogen-inducible promoters.

METHODS

T-DNA Mutagenesis and Mutant Characterization

The *Arabidopsis thaliana* Col-gi line ST8 (the eighth generation of line S6 reported in Xiao et al., 2003), harboring two copies of a transgene each containing both *RPW8.1* and *RPW8.2* under the control of their native promoters, developed an intermediate level of confined SHL readily visible to the naked eye at ~5 weeks after seed germination in short days (8 h of light, 16 h of dark). Plants of the eighth generation from this line were transformed with the binary vector pSLJ75515 (Jones et al., 1992) that contains the basta herbicide resistance gene for selection of transformants. Approximately 20,000 independent transgenic T1 plants were obtained, and the seeds were collected in 40 pools (~500 T1 lines per pool). We screened ~80,000 T2 plants (~2000 for each pool) and identified >20 mutants belonging to at least five complementation groups with accelerated SHL in 2 to 3 weeks after seed germination. The T-DNA in *erh1*/ST8 was located by inverse PCR. Specifically, the genomic DNA of the mutant was digested with *Asel* and then self-ligated using T4 DNA ligase (New England Biolabs). PCR amplification of the T-DNA-genomic DNA junction was done using the primers 5'-CGGGCCTAACTTTGGTGTGATGA-3' and 5'-CCCCCATCGTAGGTGAAGGTGA-3', designed based on the right T-DNA border of pSLJ75515. The specific PCR product was sequenced, and the T-DNA junctions in *At2g37940* (*ERH1*) were determined by PCR with gene-specific primers and primers based on the left or right border of the vector.

Unless otherwise indicated, seeds were sown in Sunshine Mix 1 (Maryland Plant and Supplies) and cold-treated (4°C for 2 d), and seedlings were kept under 22°C, 75% RH, short-day (8 h of light at ~125 $\mu\text{mol}\cdot\text{m}^{-2}\cdot\text{s}^{-1}$, 16 h of dark) conditions for 5 weeks before pathogen inoculation or other treatments. The method for plant growth in MS agar

medium was essentially the same as reported (Xiao et al., 2003). Briefly, surface-sterilized seeds were placed on MS agar plates (100 × 20 mm). After cold treatment (4°C for 2 d), the plates were placed in a growth chamber with the same growth conditions mentioned above except that the RH was slightly higher (85 to 90%) on the plates.

Introduction of *NahG*, *pad4-1*, or *acd5* into *erh1*/Col-gi or *erh1*/S5 was done by crossing. Primers for genotyping *NahG* and *pad4-1* were described by Xiao et al. (2005). To make the *erh1*/*acd5* double mutant, *erh1*/Col-gi was crossed with *acd5*/Col-0, and F2 individuals homozygous for *erh1*/*acd5* were identified by PCR for the T-DNA inserted in *ERH1* and sequencing for the point mutation in ACD5 (Liang et al., 2003).

Pathogen Strains, Inoculation, and Phenotyping

Powdery mildew isolate *Golovinomyces cichoracearum* UCSC1 was maintained on live *eds1-2* or *pad4-1* plants. Inoculation, visual scoring, and quantification of disease susceptibility were done as described previously (Xiao et al., 2005). For bacterial infection, fully expanded leaves were infiltrated with a suspension (OD₆₀₀ = 0.0002) of *Pseudomonas syringae* pv *maculicola* ES4326 wild-type strain or the avirulent strain carrying *avrRpm1* in 10 mM MgCl₂. Quantification of bacterial growth was according to Wang et al. (2007).

DNA Constructs and Gene Expression

The genomic sequence of *ERH1* was amplified by 5'-CACCGGATCCATGACACTTTATATTCGTCGTGAA-3' and 5'-CCGAATTCACGCGCCATTCATTGTGTT-3', digested with *Bam*HI and *Eco*RI, and cloned into the *Bam*HI-*Eco*RI site of binary vector pSMB under the control of the 35S promoter. An *Agrobacterium tumefaciens* strain containing 35S:*ERH1* in pSMB was used to transform *erh1*/ST8. Selection of transgenic lines was based on suppression of *erh1*-mediated strong SHL at 2 weeks old and confirmed by PCR. To express *ERH1* from the native promoter, a genomic fragment containing the coding sequence of *ERH1* was amplified by 5'-CACCGGATCCATGACACTTTATATTCGTCGTGAA-3' and 5'-CCGAGCTCACGCGCCATTCATTGTGTT-3' and cloned into the *Pst*I-*Bam*HI site of pPZP211. Then, an ~1.8-kb sequence 5' upstream of the *ERH1* start codon was amplified by 5'-CACCTGCAGACTTGTTCC-TATTTCCGATA-3' and 5'-CTCGGATCCTTATTATTCTTGTTGTTGATGATGT-3' and cloned into the *Bam*HI-*Sac*I site of the pPZP211 plasmid containing the *ERH1* coding sequence. The construct was introduced into *erh1*/S5 and *erh1*/ST8 by *Agrobacterium*-mediated transformation (Clough and Bent, 1998). To silence *ERH1* in *Arabidopsis*, *ERH1* was amplified by 5'-CACCGGATCCATGACACTTTATATTCGTCGTGAA-3' and 5'-CCGAATTCACGCGCCATTCATTGTGTT-3' and cloned to the PENTR/D-TOPO vector (Invitrogen). The fragment was then recombined into the binary Gateway vector pJawohl8 (Feys et al., 2005) using the manufacturer's suggested methods (Invitrogen) and subsequently introduced into Col-0 and ST8 by *Agrobacterium*-mediated stable transformation. For subcellular localization studies, the *ERH1* coding sequence was amplified by 5'-GGGGATCCGATGACACTTTATATTCGTCGTGAA-3' and 5'-TTGGATCCGCCATTCATTGTGTTATCCGT-3' and cloned into binary vector pBamEYFP (Wang et al., 2007) such that *YFP* was translationally fused with *ERH1* at the C terminus, resulting in pERH1-YFP. This 35S:*ERH1*-*YFP* construct was introduced into Col-0 and *erh1*/S5 by *Agrobacterium*-mediated transformation or into onion (*Allium cepa*) epidermal cells by bombardment. For colocalization analysis, the *DsRed* coding sequence was amplified with primers 5'-TAGGATCCATGGCC-TCCTCCGAGG-3' and 5'-AAAGATCTCCGCTACAGGAACAGGTG-GTG-3' and used to replace *YFP* in pERH1-YFP, resulting in pERH1-DsRed. Plasmid DNA for 35S:*ERH1*-*DsRed* was cobombarded with plasmid DNA for 35S:*mCherry*-*AtWAK2*-*HEDL* (Nelson et al., 2007), 35S:*ERD2*-*GFP* (daSilva et al., 2004), and 35S:*GFP*-*SYP42* or 35S:*GFP*-*SYP61* (Sanderfoot et al., 2001; Uemura et al., 2004) into leaves

of Col-0, followed by examination with a laser scanning confocal microscope according to a previous report (Wang et al., 2007). To silence a rice homolog of *ERH1* (Os01g0850100) by RNAi, the rice cDNA fragment was amplified by primers 5'-CACCATGGCGGTTTACATCGCTCGGGA-3' and 5'-TCATGTGCCATTGGGAGTGGCATC-3', cloned to pENTR/D-TOPO vector (Invitrogen), and then shuttled to the binary vector pANDA under the control of the ubiquitin promoter (Qu et al., 2006). The RNAi construct was introduced into *Agrobacterium* strain LBA4404, and rice transgenic plants were generated according to a previously published protocol (Qu et al., 2006).

Transcript Analysis

RNA extraction and gel blot analysis were conducted as described previously (Xiao et al., 2005). Quantification of the transcripts of *ERH1* by real-time RT-PCR was done according to Xiao et al. (2003). *ACT2* was chosen as the normalization standard for TaqMan analysis because of its constitutive expression in nearly all vegetative tissues (An et al., 1996) and its stable expression after pathogen challenge (Feys et al., 2001). cDNA-specific primers were used to measure levels of *ACT2* and *ERH1* transcripts. The sequences of the primers for *ERH1* were 5'-CCGGGACCGACACTTCAG-3' and 5'-CGGTTTCACATTATGTAGCTTCTCTCTT-3', and the sequence for the probe was 5'-ATCTTGGCTTCTTCTTCTTCCGGAGCTTG-3'. PCR was performed on an ABI 7300 sequence detection system (Applied Biosystems). Triplicate cDNA samples were prepared and analyzed for each genotype/treatment.

Yeast Strains, Vectors, and IPCS Assays

For genetic complementation tests with yeast strains lacking the IPCS gene, *AUR1*, the *ERH1* coding sequence was PCR-amplified from an *Arabidopsis* cDNA library (Paul et al., 2006) and inserted into the *SalI* site of the yeast expression vector pADH1-LEU2 to generate pERH1. Sequence-confirmed pERH1 was introduced into the yeast *aur1*Δ mutant harboring the pRS316-*AUR1* plasmid, and transformants were selected on medium lacking Leu and then transferred to YPD medium to allow for loss of pRS316-*AUR1*. Transformants that had lost the *URA3*⁺-marked pRS316-*AUR1* plasmid were selected on FOA. pERH1 was similarly introduced into the yeast *aur1*Δ/*scs7*Δ and *aur1*Δ/*sur2*Δ double mutants (Haak et al., 1997) to determine the spectrum of ceramide substrates that could be utilized by ERH1 in yeast. To assay for IPCS activities, microsomes from yeast cells expressing ERH1 were prepared as described previously (Paul et al., 2006) and analyzed for IPCS activity using PHS-, DHS-, and sphingosine-containing NBD C6-ceramides as described previously (Figueiredo et al., 2005).

In Vitro Assay of Plant IPCS Activity

Leaves (~250 mg) from 6- to 8-week-old plants were homogenated in 4 volumes of buffer (10 mM HEPES, pH 7.8, 2 mM EDTA, 2 mM β-mercaptoethanol, and plant protease inhibitor cocktail [Sigma-Aldrich]) using a Kontes glass tissue grinder. The lysates were centrifuged for 90 s at 13,400g, and the resulting supernatants were used in the enzyme assay immediately or stored at -80°C. Protein concentration of the lysates was determined using the Coomassie (Bradford) protein assay reagent from Pierce. IPCS activities in lysates were assayed using 450 μM soy phosphatidylinositol and 60 μM dodecanoyl-NBD-D-*erythro*-DHS (Matreya) as substrates, 0.5 mM CHAPS, 10 mM EDTA, 100 mM Tris-HCl (pH 7.5), and 45 μL of leaf lysate (40 to 80 μg of protein) in a total volume of 100 μL. Reactions were performed at 32°C for 40 min in the dark and terminated by the addition of 1.0 mL of methanol. The fluorescent IPC product was recovered by partitioning against *tert*-butyl methyl ether and water as described previously (Nagiec et al., 1997) and quantified by monitoring fluorescence at excitation and emission wavelengths of 466 and 537 nm,

respectively. Assay tubes having all components but terminated with methanol prior to incubation were used as controls.

Other Analysis

Sphingolipids were extracted and measured as described previously (Markham and Jaworski, 2007) except that sphingolipids were separated using a 3.0- × 100-mm, 3.5-μm silica XBD-C18 column (Agilent Technologies). Sequence alignment was done using the AlignX function of the Vector NTI software package (Invitrogen). For SA analysis, leaves of 7-week-old plants grown in short days were used to measure SA levels using a protocol described previously (Vanacker et al., 2001). Three replicates of each genotype were analyzed. This experiment was repeated three times with similar results. Trypan blue staining for cell death was performed according to Xiao et al. (2003). Laser scanning confocal imaging was done as described by Wang et al. (2007).

Accession Numbers

Sequence data from this article can be found in the Arabidopsis Genome Initiative or GenBank/EMBL databases under the following accession numbers: At ERH1 (At2g37940); At ERHL1 (At2g29525); At ERHL2 (At3g54020); Os ERH1 (Os01g0850100); AUR1P (NP_012922); Lm IPCS (XP_843601); Hs SMS1 (NP_671512); Hs SMS2 (NP_689834); ACT2 (AT3G18780); and, for EST clones: AI486724 (tomato); CX548769 (soybean); CO128855 (cotton); and CV780701 (wheat).

Supplemental Data

The following materials are available in the online version of this article.

Supplemental Figure 1. *erh1/Col-gI* Plants Are Not More Resistant to *P. syringae*.

Supplemental Figure 2. Evolution and Diversification of IPCSs (SMSs).

Supplemental Figure 3. Levels of Sphingolipids in Wild Type and *erh1* Mutant Plants.

Supplemental Figure 4. Expression and Subcellular Localization of ERH1.

Supplemental Figure 5. *ERH1* Is Not Significantly Induced by SA.

Supplemental Data Set 1. Sequence Alignment of ERH1 and Its Homologs in *Arabidopsis*, Yeast, Protozoan, and Human.

ACKNOWLEDGMENTS

We thank Jean Greenberg (University of Chicago) for seeds of *acd5*, Hua Lu (University of Maryland, Baltimore County) for advice on SA measurement, Robert Dickson (University of Kentucky) for advice on earlier yeast work in the Xiao laboratory, Jane Parker and Dieter Becker (Max Planck Institute for Plant Breeding Research) for the pJawohl8 vector, James Culver (University of Maryland, College Park) for the 35S: *ERD2-GFP* plasmid, Masa Sato (Kyoto Prefectural University) for the 35S: *GFP-SYP42* and 35S: *GFP-SYP61* constructs, Undral Orgil for technical support, and Richelle Green and Lori Urban for assistance with mutant screens and maintaining plant growth facilities. This work was supported by the start-up fund from the University of Maryland Biotechnology Institute, by the National Research Initiative of the U.S. Department of Agriculture (Grant 2006-35301-16883 to S.X.), by National Science Foundation 2010 Program funds (Grant MCB-0313466 to T.M.D. and Grant MCB-0312864 to D.V.L.), and by the Howard Hughes Medical Institute program for support of undergraduates (to D.V.L.).

Received April 13, 2008; revised October 14, 2008; accepted October 21, 2008; published November 11, 2008.

REFERENCES

- An, Y.Q., McDowell, J.M., Huang, S., McKinney, E.C., Chambliss, S., and Meagher, R.B. (1996). Strong, constitutive expression of the Arabidopsis *ACT2/ACT8* actin subclass in vegetative tissues. *Plant J.* **10**: 107–121.
- Bae, H., Kim, M.S., Sicher, R.C., Bae, H.J., and Bailey, B.A. (2006). Necrosis- and ethylene-inducing peptide from *Fusarium oxysporum* induces a complex cascade of transcripts associated with signal transduction and cell death in Arabidopsis. *Plant Physiol.* **141**: 1056–1067.
- Balague, C., Lin, B., Alcon, C., Flottes, G., Malmstrom, S., Kohler, C., Neuhaus, G., Pelletier, G., Gaymard, F., and Roby, D. (2003). HLM1, an essential signaling component in the hypersensitive response, is a member of the cyclic nucleotide-gated channel ion channel family. *Plant Cell* **15**: 365–379.
- Brodersen, P., Petersen, M., Pike, H.M., Olszak, B., Skov, S., Odum, N., Jorgensen, L.B., Brown, R.E., and Mundy, J. (2002). Knockout of Arabidopsis *ACCELERATED-CELL-DEATH11* encoding a sphingosine transfer protein causes activation of programmed cell death and defense. *Genes Dev.* **16**: 490–502.
- Bromley, P.E., Li, Y.O., Murphy, S.M., Sumner, C.M., and Lynch, D.V. (2003). Complex sphingolipid synthesis in plants: characterization of inositolphosphorylceramide synthase activity in bean microsomes. *Arch. Biochem. Biophys.* **417**: 219–226.
- Carter, H.E., Celmer, W.D., Galanos, D.S., Gigg, R.H., Lands, W.E.M., Law, J.H., Mueller, K.L., Nakayama, T., Tomizawa, H.H., and Weber, E. (1958). Biochemistry of the sphingolipides. 10. Phytoglycolipide, a complex phytosphingosine-containing lipide from plant seeds. *J. Am. Oil Chem. Soc.* **35**: 335–343.
- Clough, S.J., and Bent, A.F. (1998). Floral dip: A simplified method for *Agrobacterium*-mediated transformation of *Arabidopsis thaliana*. *Plant J.* **16**: 735–743.
- Clough, S.J., Fengler, K.A., Yu, I.C., Lippok, B., Smith, R.K., Jr., and Bent, A.F. (2000). The Arabidopsis *dnd1* “defense, no death” gene encodes a mutated cyclic nucleotide-gated ion channel. *Proc. Natl. Acad. Sci. USA* **97**: 9323–9328.
- Dangl, J.L., and Jones, J.D.G. (2001). Plant pathogens and integrated defence responses to infection. *Nature* **411**: 826–833.
- daSilva, L.L., Snapp, E.L., Denecke, J., Lippincott-Schwartz, J., Hawes, C., and Brandizzi, F. (2004). Endoplasmic reticulum export sites and Golgi bodies behave as single mobile secretory units in plant cells. *Plant Cell* **16**: 1753–1771.
- Denny, P.W., Shams-Eldin, H., Price, H.P., Smith, D.F., and Schwarz, R.T. (2006). The protozoan inositol phosphorylceramide synthase: A novel drug target that defines a new class of sphingolipid synthase. *J. Biol. Chem.* **281**: 28200–28209.
- Denny, P.W., and Smith, D.F. (2004). Rafts and sphingolipid biosynthesis in the kinetoplast parasitic protozoa. *Mol. Microbiol.* **53**: 725–733.
- Desai, K., Sullards, M.C., Allegood, J., Wang, E., Schmelz, E.M., Hartl, M., Humpf, H.U., Liotta, D.C., Peng, Q., and Merrill, A.H., Jr. (2002). Fumonisin and fumonisin analogs as inhibitors of ceramide synthase and inducers of apoptosis. *Biochim. Biophys. Acta* **1585**: 188–192.
- Ding, T., Li, Z., Hailemariam, T., Mukherjee, S., Maxfield, F.R., Wu, M., and Jiang, X.C. (2008). SMS overexpression and knockdown: Impact on cellular sphingomyelin and diacylglycerol metabolism, and cell apoptosis. *J. Lipid Res.* **49**: 376–385.
- Does, M.P., Dekker, B.M., de Groot, M.J., and Offringa, R. (1991). A quick method to estimate the T-DNA copy number in transgenic plants at an early stage after transformation, using inverse PCR. *Plant Mol. Biol.* **17**: 151–153.
- Dunn, T.M., Lynch, D.V., Michaelson, L.V., and Napier, J.A. (2004). A post-genomic approach to understanding sphingolipid metabolism in *Arabidopsis thaliana*. *Ann. Bot. (Lond.)* **93**: 483–497.
- Epple, P., Mack, A.A., Morris, V.R., and Dangl, J.L. (2003). Antagonistic control of oxidative stress-induced cell death in Arabidopsis by two related, plant-specific zinc finger proteins. *Proc. Natl. Acad. Sci. USA* **100**: 6831–6836.
- Falk, A., Feys, B.J., Frost, L.N., Jones, J.D., Daniels, M.J., and Parker, J.E. (1999). EDS1, an essential component of *R* gene-mediated disease resistance in Arabidopsis has homology to eukaryotic lipases. *Proc. Natl. Acad. Sci. USA* **96**: 3292–3297.
- Feys, B.J., Moisan, L.J., Newman, M.A., and Parker, J.E. (2001). Direct interaction between the Arabidopsis disease resistance signaling proteins, EDS1 and PAD4. *EMBO J.* **20**: 5400–5411.
- Feys, B.J., Wiermer, M., Bhat, R.A., Moisan, L.J., Medina-Escobar, N., Neu, C., Cabral, A., and Parker, J.E. (2005). Arabidopsis SENESCENCE-ASSOCIATED GENE101 stabilizes and signals within an ENHANCED DISEASE SUSCEPTIBILITY1 complex in plant innate immunity. *Plant Cell* **17**: 2601–2613.
- Figueiredo, J.M., Dias, W.B., Mendonca-Previato, L., Previanto, J.O., and Heise, N. (2005). Characterization of the inositol phosphorylceramide synthase activity from *Trypanosoma cruzi*. *Biochem. J.* **387**: 519–529.
- Frye, C.A., Tang, D., and Innes, R.W. (2001). Negative regulation of defense responses in plants by a conserved MAPKK kinase. *Proc. Natl. Acad. Sci. USA* **98**: 373–378.
- Fujiwara, S., Tanaka, N., Kaneda, T., Takayama, S., Isogai, A., and Che, F.S. (2004). Rice cDNA microarray-based gene expression profiling of the response to flagellin perception in cultured rice cells. *Mol. Plant Microbe Interact.* **17**: 986–998.
- Grant, M.R., Godiard, L., Straube, E., Ashfield, T., Lewald, J., Sattler, A., Innes, R.W., and Dangl, J.L. (1995). Structure of the Arabidopsis *RPM1* gene enabling dual specificity disease resistance. *Science* **269**: 843–846.
- Greenberg, J.T., Silverman, F.P., and Liang, H. (2000). Uncoupling salicylic acid-dependent cell death and defense-related responses from disease resistance in the Arabidopsis mutant *acd5*. *Genetics* **156**: 341–350.
- Haak, D., Gable, K., Beeler, T., and Dunn, T. (1997). Hydroxylation of *Saccharomyces cerevisiae* ceramides requires Sur2p and Scs7p. *J. Biol. Chem.* **272**: 29704–29710.
- Hakomori, S. (1983). Chemistry of glycosphingolipids. In *Handbook of Lipid Research*, Vol. 3, Sphingolipid Biochemistry J.N. Kanfer and S. Hakomori, eds (New York: Plenum Press), pp. 1–164.
- Hammond-Kosack, K.E., and Parker, J.E. (2003). Deciphering plant-pathogen communication: Fresh perspectives for molecular resistance breeding. *Curr. Opin. Biotechnol.* **14**: 177–193.
- Hanada, K., Kumagai, K., Yasuda, S., Miura, Y., Kawano, M., Fukasawa, M., and Nishijima, M. (2003). Molecular machinery for non-vesicular trafficking of ceramide. *Nature* **426**: 803–809.
- He, X., Anderson, J.C., del Pozo, O., Gu, Y.Q., Tang, X., and Martin, G.B. (2004). Silencing of subfamily I of protein phosphatase 2A catalytic subunits results in activation of plant defense responses and localized cell death. *Plant J.* **38**: 563–577.
- Huitema, K., van den Dikkenberg, J., Brouwers, J.F., and Holthuis, J.C. (2004). Identification of a family of animal sphingomyelin synthases. *EMBO J.* **23**: 33–44.
- Jirage, D., Tootle, T.L., Reuber, T.L., Frost, L.N., Feys, B.J., Parker, J.E., Ausubel, F.M., and Glazebrook, J. (1999). *Arabidopsis thaliana*

- PAD4* encodes a lipase-like gene that is important for salicylic acid signaling. *Proc. Natl. Acad. Sci. USA* **96**: 13583–13588.
- Jones, J.D., Shlumukov, L., Carland, F., English, J., Scofield, S.R., Bishop, G.J., and Harrison, K.** (1992). Effective vectors for transformation, expression of heterologous genes, and assaying transposon excision in transgenic plants. *Transgenic Res.* **1**: 285–297.
- Jurkowski, G.I., Smith, R.K., Jr., Yu, I.C., Ham, J.H., Sharma, S.B., Klessig, D.F., Fengler, K.A., and Bent, A.F.** (2004). *Arabidopsis DND2*, a second cyclic nucleotide-gated ion channel gene for which mutation causes the “defense, no death” phenotype. *Mol. Plant Microbe Interact.* **17**: 511–520.
- Kachroo, A., Venugopal, S.C., Lapchyk, L., Falcone, D., Hildebrand, D., and Kachroo, P.** (2004). Oleic acid levels regulated by glycerolipid metabolism modulate defense gene expression in *Arabidopsis*. *Proc. Natl. Acad. Sci. USA* **101**: 5152–5157.
- Kachroo, P., Shanklin, J., Shah, J., Whittle, E.J., and Klessig, D.F.** (2001). A fatty acid desaturase modulates the activation of defense signaling pathways in plants. *Proc. Natl. Acad. Sci. USA* **98**: 9448–9453.
- Kaul, K., and Lester, R.L.** (1975). Characterization of inositol-containing phosphosphingolipids from tobacco-leaves: Isolation and identification of two novel, major lipids: N-Acetylglucosamidoglucuronidoinositol phosphorylceramide and glucosamidoglucuronidoinositol phosphorylceramide. *Plant Physiol.* **55**: 120–129.
- Kliebenstein, D.J., Dietrich, R.A., Martin, A.C., Last, R.L., and Dangl, J.L.** (1999). LSD1 regulates salicylic acid induction of copper zinc superoxide dismutase in *Arabidopsis thaliana*. *Mol. Plant Microbe Interact.* **12**: 1022–1026.
- Lei, X., Zhang, S., Bohrer, A., Bao, S., Song, H., and Ramanadham, S.** (2007). The group VIA calcium-independent phospholipase A2 participates in ER stress-induced INS-1 insulinoma cell apoptosis by promoting ceramide generation via hydrolysis of sphingomyelins by neutral sphingomyelinase. *Biochemistry* **46**: 10170–10185.
- Levine, T.P., Wiggins, C.A., and Munro, S.** (2000). Inositol phosphorylceramide synthase is located in the Golgi apparatus of *Saccharomyces cerevisiae*. *Mol. Biol. Cell* **11**: 2267–2281.
- Liang, H., Yao, N., Song, J.T., Luo, S., Lu, H., and Greenberg, J.T.** (2003). Ceramides modulate programmed cell death in plants. *Genes Dev.* **17**: 2636–2641.
- Liu, Y., Schiff, M., Czymmek, K., Tallóczy, Z., Levine, B., and Dinesh-Kumar, S.P.** (2005). Autophagy regulates programmed cell death during the plant innate immune response. *Cell* **121**: 567–577.
- Lorrain, S., Lin, B., Auriac, M.C., Kroj, T., Saindrenan, P., Nicole, M., Balague, C., and Roby, D.** (2004). Vascular associated death1, a novel GRAM domain-containing protein, is a regulator of cell death and defense responses in vascular tissues. *Plant Cell* **16**: 2217–2232.
- Lorrain, S., Vaillau, F., Balague, C., and Roby, D.** (2003). Lesion mimic mutants: Keys for deciphering cell death and defense pathways in plants? *Trends Plant Sci.* **8**: 263–271.
- Lynch, D.V., and Dunn, T.M.** (2004). An introduction to plant sphingolipids and a review of recent advances in understanding their metabolism and function. *New Phytol.* **161**: 677–702.
- Mach, J.M., Castillo, A.R., Hoogstraten, R., and Greenberg, J.T.** (2001). The *Arabidopsis*-accelerated cell death gene *ACD2* encodes red chlorophyll catabolite reductase and suppresses the spread of disease symptoms. *Proc. Natl. Acad. Sci. USA* **98**: 771–776.
- Marggraf, W.D., and Kanfer, J.N.** (1984). The phosphorylcholine acceptor in the phosphatidylcholine:ceramide cholinephosphotransferase reaction. Is the enzyme a transferase or a hydrolase? *Biochim. Biophys. Acta* **793**: 346–353.
- Markham, J.E., and Jaworski, J.G.** (2007). Rapid measurement of sphingolipids from *Arabidopsis thaliana* by reversed-phase high-performance liquid chromatography coupled to electrospray ionization tandem mass spectrometry. *Rapid Commun. Mass Spectrom.* **21**: 1304–1314.
- Markham, J.E., Li, J., Cahoon, E.B., and Jaworski, J.G.** (2006). Separation and identification of major plant sphingolipid classes from leaves. *J. Biol. Chem.* **281**: 22684–22694.
- Meng, A., Luberto, C., Meier, P., Bai, A., Yang, X., Hannun, Y.A., and Zhou, D.** (2004). Sphingomyelin synthase as a potential target for D609-induced apoptosis in U937 human monocytic leukemia cells. *Exp. Cell Res.* **292**: 385–392.
- Nagiec, M.M., Nagiec, E.E., Baltisberger, J.A., Wells, G.B., Lester, R.L., and Dickson, R.C.** (1997). Sphingolipid synthesis as a target for antifungal drugs. Complementation of the inositol phosphorylceramide synthase defect in a mutant strain of *Saccharomyces cerevisiae* by the *AUR1* gene. *J. Biol. Chem.* **272**: 9809–9817.
- Nawrath, C., Heck, S., Parinthewong, N., and Metraux, J.P.** (2002). EDS5, an essential component of salicylic acid-dependent signaling for disease resistance in *Arabidopsis*, is a member of the MATE transporter family. *Plant Cell* **14**: 275–286.
- Nelson, B.K., Cai, X., and Nebenfuhr, A.** (2007). A multicolored set of in vivo organelle markers for co-localization studies in *Arabidopsis* and other plants. *Plant J.* **51**: 1126–1136.
- Neuwald, A.F.** (1997). An unexpected structural relationship between integral membrane phosphatases and soluble haloperoxidases. *Protein Sci.* **6**: 1764–1767.
- Nishimura, M.T., Stein, M., Hou, B.H., Vogel, J.P., Edwards, H., and Somerville, S.C.** (2003). Loss of a callose synthase results in salicylic acid-dependent disease resistance. *Science* **301**: 969–972.
- Orgil, U., Araki, H., Tangchaiburana, S., Berkey, R., and Xiao, S.** (2007). Intraspecific genetic variations, fitness cost and benefit of *RPW8*, a disease resistance locus in *Arabidopsis thaliana*. *Genetics* **176**: 2317–2333.
- Paul, S., Gable, K., Beaudoin, F., Cahoon, E., Jaworski, J., Napier, J.A., and Dunn, T.M.** (2006). Members of the *Arabidopsis* FAE1-like 3-ketoacyl-CoA synthase gene family substitute for the Elop proteins of *Saccharomyces cerevisiae*. *J. Biol. Chem.* **281**: 9018–9029.
- Pettus, B.J., Chalfant, C.E., and Hannun, Y.A.** (2002). Ceramide in apoptosis: An overview and current perspectives. *Biochim. Biophys. Acta* **1585**: 114–125.
- Phan, V.H., Herr, D.R., Panton, D., Fyrst, H., Saba, J.D., and Harris, G.L.** (2007). Disruption of sphingolipid metabolism elicits apoptosis-associated reproductive defects in *Drosophila*. *Dev. Biol.* **309**: 329–341.
- Pruzinska, A., Tanner, G., Anders, I., Roca, M., and Hortensteiner, S.** (2003). Chlorophyll breakdown: Pheophorbide a oxygenase is a Rieske-type iron-sulfur protein, encoded by the *ACCELERATED CELL DEATH 1* gene. *Proc. Natl. Acad. Sci. USA* **100**: 15259–15264.
- Qu, S., Liu, G., Zhou, B., Bellizzi, M., Zeng, L., Dai, L., Han, B., and Wang, G.L.** (2006). The broad-spectrum blast resistance gene *Pi9* encodes a nucleotide-binding site-leucine-rich repeat protein and is a member of a multigene family in rice. *Genetics* **172**: 1901–1914.
- Sanchez, A.M., Malagarie-Cazenave, S., Olea, N., Vara, D., Chiloeches, A., and Diaz-Laviada, I.** (2007). Apoptosis induced by capsaicin in prostate PC-3 cells involves ceramide accumulation, neutral sphingomyelinase, and JNK activation. *Apoptosis* **12**: 2013–2024.
- Sanderfoot, A.A., Kovaleva, V., Bassham, D.C., and Raikhel, N.V.** (2001). Interactions between syntaxins identify at least five SNARE complexes within the Golgi/prevacuolar system of the *Arabidopsis* cell. *Mol. Biol. Cell* **12**: 3733–3743.
- Stein, M., Dittgen, J., Sanchez-Rodriguez, C., Hou, B.H., Molina, A., Schulze-Lefert, P., Lipka, V., and Somerville, S.** (2006). *Arabidopsis* PEN3/PDR8, an ATP binding cassette transporter, contributes to nonhost resistance to inappropriate pathogens that enter by direct penetration. *Plant Cell* **18**: 731–746.

- Tafesse, F.G., Huitema, K., Hermansson, M., van der Poel, S., van den Dikkenberg, J., Uphoff, A., Somerharju, P., and Holthuis, J.C.** (2007). Both sphingomyelin synthases SMS1 and SMS2 are required for sphingomyelin homeostasis and growth in human HeLa cells. *J. Biol. Chem.* **282**: 17537–17547.
- Tang, D., Ade, J., Frye, C.A., and Innes, R.W.** (2005). Regulation of plant defense responses in *Arabidopsis* by EDR2, a PH and START domain-containing protein. *Plant J.* **44**: 245–257.
- Tian, A.G., et al** (2004). Characterization of soybean genomic features by analysis of its expressed sequence tags. *Theor. Appl. Genet.* **108**: 903–913.
- Uemura, T., Ueda, T., Ohniwa, R.L., Nakano, A., Takeyasu, K., and Sato, M.H.** (2004). Systematic analysis of SNARE molecules in *Arabidopsis*: Dissection of the post-Golgi network in plant cells. *Cell Struct. Funct.* **29**: 49–65.
- Ullman, M.D., and Radin, N.S.** (1974). The enzymatic formation of sphingomyelin from ceramide and lecithin in mouse liver. *J. Biol. Chem.* **249**: 1506–1512.
- Vanacker, H., Lu, H., Rate, D.N., and Greenberg, J.T.** (2001). A role for salicylic acid and NPR1 in regulating cell growth in *Arabidopsis*. *Plant J.* **28**: 209–216.
- Voelker, D.R., and Kennedy, E.P.** (1982). Cellular and enzymic synthesis of sphingomyelin. *Biochemistry* **21**: 2753–2759.
- Vorwerk, S., Schiff, C., Santamaria, M., Koh, S., Nishimura, M., Vogel, J., Somerville, C., and Somerville, S.** (2007). *EDR2* negatively regulates salicylic acid-based defenses and cell death during powdery mildew infections of *Arabidopsis thaliana*. *BMC Plant Biol.* **7**: 35.
- Waggoner, D.W., Xu, J., Singh, I., Jasinska, R., Zhang, Q.X., and Brindley, D.N.** (1999). Structural organization of mammalian lipid phosphate phosphatases: Implications for signal transduction. *Biochim. Biophys. Acta* **1439**: 299–316.
- Wang, H., Li, J., Bostock, R.M., and Gilchrist, D.G.** (1996a). Apoptosis: A functional paradigm for programmed plant cell death induced by a host-selective phytotoxin and invoked during development. *Plant Cell* **8**: 375–391.
- Wang, W., Devoto, A., Turner, J.G., and Xiao, S.** (2007). Expression of the membrane-associated resistance protein RPW8 enhances basal defense against biotrophic pathogens. *Mol. Plant Microbe Interact.* **20**: 966–976.
- Wang, W., Jones, C., Ciacci-Zanella, J., Holt, T., Gilchrist, D.G., and Dickman, M.B.** (1996b). Fumonisin and *Alternaria alternata lycopersici* toxins: Sphinganine analog mycotoxins induce apoptosis in monkey kidney cells. *Proc. Natl. Acad. Sci. USA* **93**: 3461–3465.
- Xiao, S., Brown, S., Patrick, E., Brearley, C., and Turner, J.G.** (2003). Enhanced transcription of the *Arabidopsis* disease resistance genes *RPW8.1* and *RPW8.2* via a salicylic acid-dependent amplification circuit is required for hypersensitive cell death. *Plant Cell* **15**: 33–45.
- Xiao, S., Calis, O., Patrick, E., Zhang, G., Charoenwattana, P., Muskett, P., Parker, J.E., and Turner, J.G.** (2005). The atypical resistance gene, *RPW8*, recruits components of basal defence for powdery mildew resistance in *Arabidopsis*. *Plant J.* **42**: 95–110.
- Xiao, S., Ellwood, S., Calis, O., Patrick, E., Li, T., Coleman, M., and Turner, J.G.** (2001). Broad-spectrum mildew resistance in *Arabidopsis thaliana* mediated by *RPW8*. *Science* **291**: 118–120.
- Xiao, S., Ellwood, S., Findlay, K., Oliver, R.P., and Turner, J.G.** (1997). Characterization of three loci controlling resistance of *Arabidopsis thaliana* accession Ms-0 to two powdery mildew diseases. *Plant J.* **12**: 757–768.